

Reinforcement Learning for Control of Evolutionary and Ecological Processes

Bryce Allen Bagley^{1,2,3,*}, Navin Khosninan^{1,2}, and Claudia K Petritsch^{1,2,4,5}

¹Mathematical Medicine Group, Stanford University, Stanford, CA 94305, USA

²Department of Neurosurgery, Stanford Medical School, Stanford, CA 94305, USA

³Physician-Scientist Training Program, Stanford Medical School, Stanford, CA 94305, USA

⁴Maternal & Child Health Research Institute, Stanford University School of Medicine, Stanford, CA 94305, USA

⁵Stanford Cancer Institute, Stanford University School of Medicine, Stanford, CA 94305, USA

*Correspondence: bbagley@stanford.edu

SUMMARY

As research in evolutionary dynamics and Evolutionary Game Theory moves from the realm of theory into application in oncology, algorithms that account for physiologic variation are needed to move beyond simple models. Yet few algorithms exist that integrate these ecological and physiological factors which are central to evolution in biological systems. We introduce a new model of evolutionary games which accounts for ecology and physiology by framing both as computations. Leveraging this new model, we develop an algorithmic approach for controlling evolution via methods from Reinforcement Learning, a branch of Machine Learning, and prove rigorous algorithmic bounds on the complexity of solving this problem. This approach enables us to obtain first-of-their-kind results on the algorithmic problem of learning to control an evolving population of cells. We prove a complexity bound on controlling evolution in situations with limited prior knowledge of cellular physiology or ecology, give the first results on the most general version of the mathematical problem of directed evolution, and establish a new link between AI and biology.

KEYWORDS

reinforcement learning, evolution, evolutionary dynamics, artificial intelligence, evolutionary game theory, quantitative oncology, mathematical oncology

INTRODUCTION

In medical contexts, the clearest application of *Evolutionary Game Theory* (EGT).^{1–7} is to modeling the physiology of cancers and their responses to therapies with the goal to optimize cancer treatment.^{7–11} There is growing interest within clinical medicine regarding the possibility of applying EGT to the development and optimization of cancer therapies, immunology, and infectious disease treatment, but thus far there has been limited ability to integrate the enormous quantities of available biomedical data. In addition, there are very few studies of treatment courses with meaningful dynamics over time, particularly because of the difficulty of experimenting with combination and time-course therapies. Instead, the current standard of care in cancer is generally to use one or two chemotherapeutics along with surgery and/or radiation. If the patient is not cured, the cancer develops resistance to those drugs through multi-faceted mechanisms, and a new drug or drug combination must be used. Mechanisms of resistance include,

among others, modulation of the immune system, changes to non-coding regions which interfere with therapy efficacy, and mutations and epigenetic changes which alter features of cancer cells such as signalling pathways, drug transport into and out of cells, target site structure, and drug metabolism.¹² However, as discussed in^{3,5–7} and many others, there is growing evidence that therapies which vary over time in more strategic and complex ways have great potential to improve cancer outcomes. Similarly, bacterial and viral infections develop resistance to antibiotics and antivirals via evolutionary processes very much analogous to those in cancers.

EGT uses combined elements of the discrete games from economics, the differential games primarily from engineering, and the mathematical and biological literature on evolution and ecology to predict how evolutionary processes determine the frequencies of different types in a population.¹ In biomedical contexts, there has been particular interest in the application of EGT to the study of cancer and therapy resistance,^{3,5–7,13–15} and this is likewise our focus in this paper.

A key goal of predicting evolutionary dynamics is to be able to intervene and steer evolution towards a desired state. This would represent a quantitative form of directed evolution, an approach of artificial selection already used on bacteria to optimize biomolecular catalysts for industrial manufacturing of pharmacologics, agricultural chemicals and more.^{16–19} This is essentially an approach of applying *artificial* selection in much the same fashion that *natural* selection optimizes organisms in nature, and the existing experimental success is indicative of the possibilities which may lie in more quantitatively-driven use. Accomplishing this will require mathematical tools for guiding dynamics in a fine-grained manner, and such tools will themselves require the development of new theoretical and computational results.

Here we explore two key ideas. First, questions of how to prove a rigorous algorithmic bound on the computational problem of optimal control of evolution. Second, the duality in the nature of the underlying process as both a competition and a computation. The former has clear connections with what we discuss above about the history and present state of the cross-talk between game theory and evolutionary biology.² The latter, however, is perhaps a subtler one, and is related to a radical yet compelling proposal by Krakauer, Bertschinger, Olbrich, Flack, and Ay.²¹ They propose that individuality exists not as a binary property, but a spectral one with its origins in information theory. Instead of arbitrary human-imposed boundaries, one instead looks at how the mutual information of different partitionings varies and thus defines degrees of individuality. This will be discussed further in the Methods section on Computational Duality.

Our goal in this paper is to develop a novel approach which introduces new techniques into the theoretical literature of EGT while focusing on its ultimate use in experiment and application. To accomplish this, we make use of Osband and Van Roy's work on model-based reinforcement learning (RL) of Markov Decision Processes, in which they proved the first unified regret bounds for model-based RL of quadratic systems – like EGT – which to our knowledge remain state of the art to this day.^{22,23} Linking these results from the theory of artificial intelligence with the specific function classes³ of interest in EGT, we introduce and develop a mathematical formalism for an evolutionary control theory via a combination of EGT, reinforcement learning, and control systems. In addition to defining and exploring this formalism, we derive bounds on learning to control directed evolution which match the state-of-the-art bounds in the theory of artificial

¹The term "types" in EGT is a deliberately general one, as the mathematical tools can be used for the study of genotype frequencies in a population, foraging strategies in macro-organisms, cultural changes, and even collective behavior in response to economic policies.

²This conceptual view is ubiquitous in theoretical biophysics, systems biology, and adjacent fields, and a recent review article offers a helpful explanation of them in terms of potential therapeutic applications.²⁰

³A term used in machine learning and artificial intelligence to denote a collection of functions with one or more relevant properties in common.

intelligence more broadly. However, much of the value of theory comes from eventual application to practice, and as discussed by Traulsen and Glynatsi there is a growing divide between theory and practice in EGT.²⁴

In the standard formulation of EGT,^{1,2,4} one studies a vector c of q types – c_1, c_2, \dots, c_q – which interact within some environment with the goal of predicting what fraction of the total population each type will comprise over time. The interactions between types are modeled as an interaction matrix \mathbf{F} such that f_{ij} predicts how the j -th type will impact the i -th type. The unadjusted fitness of a type c_i – that is, the rate at which its population will grow – is thus defined by $\mathbf{F}_i c$, where \mathbf{F}_i is the i -th row of \mathbf{F} . Because we are concerned with what fractions of the population each type comprises, these fitnesses must be normalized. Thus, the average fitness of all types is computed via weighting by population fraction, and this is subtracted from the fitnesses of all types to normalize population growth.

While in reality populations essentially never remain static in total size, this fractional representation is far more useful for mathematical analysis and in general does not diminish the value of the analysis. The growth of a type's sub-population is proportional to its current size, so the total formulation of a basic Evolutionary Game Theory problem is as follows.

For a specific type,

$$d_t c_i = c_i \left(\left(\sum_j \mathbf{F}_{ij} c_j \right) - c^T \mathbf{F} c \right)$$

Extending to all types present, we have

$$d_t c = \mathbf{C}_a \left(\mathbf{F} c - \vec{1} c^T \mathbf{F} c \right) \quad (1)$$

Here \mathbf{C}_a is a diagonal matrix whose entries are the elements of c , defined explicitly as

$$\mathbf{C}_a = \sum_{i=1}^q \mathbf{E}_i c^T \vec{e}_i \quad (2)$$

Where here \vec{e}_i is the vector with all zero entries save for a 1 at entry i , and \mathbf{E}_i is the $q \times q$ matrix with the q -th main diagonal entry as 1 and all other entries as 0. We have subscripted this matrix \mathbf{C}_a for convenience and cleaner notation in certain more complex calculations to come.

Additionally, $c^T \mathbf{F} c$ is the scalar representing the population-fraction weighted sum of raw fitnesses of all types. This can be more understood as first computing the fitness of each type and then taking the weighted average for the population by multiplying each individual fitness by its population fraction and summing.

This general form of nonlinear dynamical system can thus be used to predict how the composition of the overall population will change over time. Extensions often account for mutations, which in the continuous case essentially transfer infinitesimal fractions of the population from one type to another, but the general principle holds.^{1,2,4,25}

If mutations are to be incorporated, this would be done via the addition of a linear mapping \mathbf{M} which describes the average rate at which each respective type mutates into any others. This mapping would be a symmetric matrix with diagonal entries $1 - \delta$, with the off-diagonal entries representing these mutations being some distribution which sums to δ .

Compared with the deeply interlinked nature of theory and data analysis within bioscience in the first half of the 20th century, comparatively little interaction occurred between them in the latter half. Despite being theoretical, EGT has still provided useful insights even in abstract yet practical contexts. It offers explanations of why intuitively strange situations in ecology can remain stable, and in recent years has seen early application to analyzing cancer progression and microbial evolution of antibiotic resistance. However, these efforts have in some ways been constrained by the methods used. In most applications the number of types q might be three or four, and the entries of \mathbf{F} will be bird's-eye-view estimates from large-scale observations of bacterial and cancer cell populations.

Bioinformatics tools which have emerged in recent decades may allow quantitative researchers to generate higher-fidelity approximations of \mathbf{F} for q large enough to make clinically relevant predictions beyond the simple test cases being assessed at present. Such work is critical, and a goal of this study is to begin the creation of a new class of tools for such researchers to use. In particular, work in the area of network inference algorithms has made it increasingly possible to estimate interaction effects within cells and between them. This represents an opportunity for a new approach to evolutionary dynamics which can make use both of contemporary methods in biomedical data sciences and of rich theory.

RESULTS

Modeling the biophysics of disease physiology across multiple scales and diverse types of transport and biochemical processes is a significant mathematical challenge. As discussed in the Methods subsection on Computational Duality, one of the new methods we introduce is to model multiple types of biophysical processes as all representing a single unifying sort of computation. For example, the conversion of one molecule into another by an enzymatic process is a computation as it changes the set of interactions the matter from the original molecule can engage in. Likewise, the movement of a molecule from a cell into the intercellular space – or vice versa – also changes the set of interactions that molecule can engage in. We introduce the term multicules to denote the units of this unifying computational representation.

Additionally, for interfacing with experimental research the model must be applicable to systems where data for values of c is readily obtained while data for values of x is more limited, even though the dynamics themselves are in truth defined in terms of x . One option is to assume a given estimate of c maps onto an estimated x (and vice versa), and have the model be a hybrid of dynamics over c and x . For the purposes of this study, the approach will be to assume a pseudo-invertible⁴ linear map $\mathbf{B}x = c$ which is time-invariant. Incorporating noise will be relevant later, so we will use the notation $\tilde{\mathbf{B}} = \mathbf{B}x + \xi$ with ξ being a vector of zero-mean noise. For the time being, however, we will assume perfect "estimates" and ignore the ξ component of $\tilde{\mathbf{B}}$. Further, we define a vector of inputs to the ecology u , and a matrix Z mapping inputs to multicules. However, it is not in fact required that we have any knowledge of \mathbf{B} , \mathbf{G} , or any other parameter matrices a priori. This is where the application of reinforcement learning will become central to later sections of the study. For now, we must first define a model of the evolutionary process. The rest of this section will be a discussion of the model and how we can convert it into a Partially Observable Markov Decision Process (POMDP) so as to enable the use of the extensive research in control systems engineering and the theory of artificial intelligence.

One would ideally like there to be a fairly straightforward means of using existing experimen-

⁴See Supplemental Information Section 1 for a discussion of the validity of the assumption of pseudo-invertability.

tal data to determine an initial model which the RL algorithm will then optimize. In what follows, we derive a model whose complexity can appear unreasonable. Indeed, our learning algorithm would produce a significantly underspecified set of matrices if it alone were used for inferring the model. The added complexity, however, is intentional and strategic for two reasons. First, it allows more direct input of known experimental values, which serve as a Bayesian prior for the model to be learned. This includes data on enzymatic reactions, estimates of the relationship between concentrations of different multicules, population fractions of different cell types, and more. Second, one can use the known values as an approximate ground truth for specifying various parameters, reducing – potentially quite substantially – the number of parameters to be derived from the model inferred via Reinforcement Learning. While this second approach may not be considered important in some use cases, it could be useful for many applications. This combination of benefits from the more mechanistic model justifies the complexity, and if a fully mechanistic model is not desired then one can simply use the full mathematical formulation for creating a sort of experiment-driven Bayesian prior over the space of possible models.

Dynamical System Model for Multicule Evolutionary Dynamics

To begin, we want to ensure the underlying mathematical model is described entirely with respect to multicule "computations" on x . As derived in Section 1 of the Supplemental Information, converting the standard EGT model to one based on multicules yields the following model.

$$d_t c = \mathbf{MC}_B^T \left(\mathbf{G}x - \vec{1}(\mathbf{B}x)^T (\mathbf{G}x) \right) + \tilde{\mathbf{Z}}u \quad (3)$$

\mathbf{C}_B^T is a matrix whose diagonals are the entries of $\mathbf{B}x$. In other words, \mathbf{C}_B is defined as

$$\mathbf{C}_B^T = \sum_{i=1}^q \mathbf{E}_i(\mathbf{B}x)^T \vec{e}_i \quad (4)$$

Our definition of \mathbf{B} is such that this would be equivalent to the earlier \mathbf{C}_a if our inferences were perfect, but this would require a perfect linear model of all molecular interactions involved – a fundamental impossibility given the nonlinearity of biological processes. Additionally, values of c – and thus \mathbf{C}_a – would be noisy estimates from data.

We note a potentially non-obvious feature of Equation (3). We refer to this model as being a quadratic dynamical system, yet it is clear that the term $\vec{1}(\mathbf{B}x)^T (\mathbf{G}x)$ is quadratic but will then be multiplied by \mathbf{C}_B – which is a function of x . However, because of the structure of the problem – as seen in the fact that we have a scalar value multiplied by $\vec{1}$ so that it will be applied to all vector elements of $d_t c$ – this is equivalent to defining an additional variable. This would be a book-keeping variable, in some sense, such that we have $\vec{1}(\mathbf{B}x)^T (\mathbf{G}x) = \vec{1}x_{\text{book}}$ separate from the actual x entries. Its dynamics would then be $d_t x_{\text{book}} = (\mathbf{B}x)^T (\mathbf{G}x)$ to preserve system structure. As a result, every component of the dynamical system is either of either linear or quadratic order. The same approach can easily be extended to the full model of Equation (8) and its equivalent 2nd-order equation.

We assume dynamics to alterations in the ecology can be approximated as some multidimensional impulse at time t_0 which decays back to a baseline. \mathbf{U} is a diagonal matrix analogous to \mathbf{C}_B , but for the vector of inputs u as

$$\mathbf{U} = \sum_{i=1}^m \mathbf{E}_i u^T \vec{e}_i \quad (5)$$

Other functional forms are of course possible, and in a wide variety of cases we anticipate that our proofs will apply equally to other models. In this study we will only analyze this particular form of ecological model because the ability to construct high-dimensional sigmoids from it allows the model to describe a broad range of ecological processes. This sigmoid model is introduced below.

192
193
194
195
196

Non-static Ecology

197
198
199
200

Additionally, we would like inputs to be able to modify the ecology of the system and physiology of the organisms within it in ways not directly captured by a mapping from u to x . To do this, we define

$$\mathbf{G}(t) = \mathbf{G}_0 + \Delta \mathbf{U} \mathbf{V} \quad (6)$$

It is important to note that the form of $\Delta \mathbf{U} \mathbf{V}$ captures modifications to the *ecology* of an evolutionary system which are separate from the direct multicules introduced via an external input into the system. The matrices Δ and \mathbf{V} are needed to reshape the dynamics of \mathbf{U} , and the three matrices in concert describe the effects of inputs on the ecological state of the model just as \mathbf{Z} describes the inputs' direct mapping to x where relevant.

201
202
203
204
205

To capture the decay process post-impulse, we use a diagonal matrix of decay rates Ξ modifying $\Delta \mathbf{U} \mathbf{V}$ into $\Delta \tilde{\mathbf{U}} e^{-\Xi t} \mathbf{V}$, and have

$$d_t \mathbf{G} = -\Delta \tilde{\mathbf{U}} \Xi e^{-\Xi t} \mathbf{V} \quad (7)$$

One can model a shift from one baseline ecology to another simply by having the midpoint between the two baselines be analogous to one impulse decaying backwards in time towards an original \mathbf{G}_0 , and a second impulse as meeting in the middle with respect to some new baseline \mathbf{G}'_0 .

208
209
210
211

If we proceed through the matrix multiplications as discussed in Supplemental Information Section 1, we derive the completed model of the evolutionary dynamics with the estimation procedures taken into account.

$$d_t x = \mathbf{B}^{-1} \mathbf{C}_B \left(\mathbf{M} \mathbf{G} x - \vec{1} (x^T \mathbf{B}^T \mathbf{G} x) \right) + \mathbf{Z} u \quad (8a)$$

$$d_t \mathbf{G} = -\Delta \tilde{\mathbf{U}} \Xi e^{-\Xi t} \mathbf{V} \quad (8b)$$

Note that \mathbf{Z} is equivalent to $\mathbf{B}^{-1} \tilde{\mathbf{Z}}$, to streamline notation. Entries of \mathbf{Z} serve to map external inputs into the multicules they become within the system, in this study according to the functional form of u as decays from a given input point. In terms of pharmaceuticals, the term including \mathbf{U} can be thought of as the effects of active drug molecules, and $\mathbf{Z} u$ as combining the rates of excretion and the rates of metabolism into pharmacologically inactive compounds. As discussed at the beginning of the Results section, this complex system of equations enables a Bayesian

215
216
217
218
219
220

prior hypothesis over the space of possible models and for the purposes of learning can readily
 221 reduce to a simpler model, which – given sufficient experimental data – can be re-expanded
 222 used as a mechanistic Bayesian posterior distribution over the space of possible models. This
 223 simpler model will be summarized using \mathbf{A} to denote the largest matrix resulting from performing
 224 all the matrix multiplications in Equation (8).
 225

POMDP for Multicule Evolutionary Models

Finally, for the sake of our later analysis, it can be useful to convert the system in Equation
 227 (8) into a single, equivalent higher-order equation. The derivation is somewhat lengthy,
 228 so it can be found in Section 1 of the Supplemental Information. The "bookkeeping variable"
 229 mentioned earlier enables us to preserve the standard property of EGT models being quadratic
 230 dynamical systems. That property will be important later, as regret bounds for model-predictive
 231 reinforcement learning are not known for all but a small number of very specific equations and a
 232 much smaller number of model classes – linear, quadratic, and generalized linear models being
 233 the only such general classes for which there are to our knowledge adequate bounds.
 234

To condense our notation for the proceeding sections, we will discretize the 2nd-order dy-
 235 namical model into a Markov Decision Process (MDP) transfer function.
 236

$$\Psi(x'|x, u) = \psi(x, u) + \vec{\xi}(x_{k+1} - x_k) \cdot (\delta t) = \frac{d^2x}{dt^2}(\delta t)^2 + \vec{\xi}(x_{k+1} - x_k) \cdot (\delta t) \quad (9)$$

with $\vec{\xi}$ a zero-mean sub-Gaussian noise vector to account for model error (and absorbing
 237 the earlier ξ term), multiplied by (δt) so that it is proportional to the time-step length. There is
 238 thus a parameter σ_ψ describing the maximum variance across entries of this sub-Gaussian noise
 239 vector. The noise is sub-Gaussian rather than Gaussian to prevent the mathematical difficulties
 240 connected with the MDP RL analysis on an unbounded range of outcomes, and this is also
 241 physically correct given conservation of mass. Because we can only observe a subset of the
 242 system's components at any given time, this MDP is termed "Partially Observable" and is thus
 243 a POMDP. Armed with this single-equation POMDP, we proceed to develop the optimal control
 244 results.
 245

Parameter Learning

Summarizing the evolutionary game using the time-evolution operator $\Psi(x(k+1)|x(k), u(k))$
 247 from Equation (27), describing how the system changes based on its present state and inputs
 248 at some time k , we can construct a Bellman function for it. The full discussion can be found in
 249 Section 2 of the Supplemental Information, but to summarize we have the following:
 250

$$V(x(k), u(k)) = L(x(\tau), u(\tau)) + \gamma \int_X dx \Psi(x(k+1)|x(k), u(k)) V(x(k+1), u(k+1)) \quad (10)$$

Here $V(\cdot, \cdot)$ is the value at a given time based on the state and input, and $L(\cdot, \cdot)$ is the reward
 251 associated with the final state which would result at time τ following a given input sequence
 252 $\{u(k), u(k+1), \dots, u(\tau)\}$ given the current state $x(k)$.
 253

The remaining key component of our derivations is the learning of parameter matrices themselves. Beginning with some set of matrices inferred from experiments, the expectation values and uncertainty in those inferences define respective prior distributions over the parameter matrices. Here we are agnostic as to the method used to generate these prior distributions.

One will inevitably need to select a subset of variables to create a Reduced-Order Model (ROM) for the POMDP Ψ , given the enormous dimensionality of the ideal approximation: a Full-Order Model incorporating all multicules involved in the system. There will be a lower bound on the error resulting from the difference between the ROM and the FOM, expressed as the residual, which is the difference between the state resulting from a ROM and that which would be seen for the same variable subset in an FOM. We denote the magnitude of this error as ε_O . A number of authors have described error bounds for various types of dynamical systems, and this continues to be an area of active research.²⁶⁻³¹ To our knowledge the best bound on this error for nonlinear dynamical systems is given by Chellappa et al in³². Their method is rather technical, and translating their error bounds to the context of our problem in detail is beyond the scope of this paper. We note the existence of such methods both to acknowledge an interesting and highly relevant body of literature, and to indicate the direction one could pursue in proving detailed bounds on ε_O . In addition, there is some fundamental error limit ε_{\min} below which a quadratic model for a given biological system could not be further optimized, regardless of whether or not it were reduced-order. Thus the problem we analyze here is more precisely one of reinforcement learning to minimize any error beyond the minimum set by those two limits, and optimal treatment selection given such an optimized model.

The error bounds for reinforcement learning of POMDPs proven across^{22,23,33} are both state of the art⁵ and highly general compared with most results in the field, which makes them very suitable for this problem. A lengthier discussion of these bounds in our case can be found in Supplemental Information Section 4, and relate specifically to the algorithm Posterior Sampling Reinforcement Learning (PSRL).²³ In summary, we use their results to derive regret for using the PSRL algorithm to both learn the parameter matrices and select inputs to optimize trajectories through evolutionary space.

Because ε_O is separate from the ξ term which we would like to minimize – the goal of using RL to improve our model – there will be a baseline accumulation of error in addition to ε_k , the error from the estimation of the integral portion of the Bellman operator. The derivation of the function describing ε_k is discussed in Section 3 of the Supplemental Information. They will be bounded by the sum of their absolute values, so we know that the error from our approximations (as opposed to the error from sub-optimal parameters, which PSRL is used to minimize) will be bounded as $\varepsilon \leq |\varepsilon_k| + |\varepsilon_O| + |\varepsilon_{\min}|$, as this would be the case if there were only constructive interference among the error values.

We use $\{\varepsilon\}$ to denote the triplet of upper bounds on the errors. First ε , the upper bound on unavoidable error. Second and third are ε_R and ε_ψ , the errors between the inferred and actual functions for each of reward and transition process. ε_R corresponds to learning the $\vec{\omega}$ for the reward function if it is not fully specified in advance, and likewise ε_ψ for learning the model Ψ .

$$\mathbb{E}[\text{reg}](T, \Psi, R, \{\varepsilon\}) = \tilde{\mathcal{O}}\left(\sqrt{T}\left[\sigma_R(m+n)\sqrt{\log\left[\frac{\|\vec{\omega}\|_2\|\{x, u\}\|_{\max}}{\varepsilon_R}\right]} + \mathbb{E}[\mathcal{K}]\sigma_\psi n\sqrt{\log\left[\frac{n\|\mathbf{A}\|_1\|\mathbf{A}\|_\infty\|x\|_{\max}}{\varepsilon_\psi}\right]}\right]\right) \quad (11)$$

⁵Per our literature review and personal communication with B. Van Roy and M. Kochenderfer.

A is a combined model parameter matrix being learned,⁶ and \tilde{r}_{eg} is the regret over all learning episodes. Because there are multiple ways of formulating the problem without altering these bounds, as discussed in Supplemental Information Section 1, we do not specify A in terms of Δ , \mathbf{V} , Ξ , \mathbf{B} , \mathbf{G} . In each case, it will still hold that $\mathbf{A} \in \mathbb{R}^{\mathcal{O}(n) \times \mathcal{O}(n)}$, so it does not impact our analysis at this level of granularity. Here $\|\mathbf{A}\|_1$ and $\|\mathbf{A}\|_\infty$ are respectively the maximum column-wise and row-wise sums in the matrix, $\|\mathbf{A}\|_2 \leq \sqrt{\|\mathbf{A}\|_1 \|\mathbf{A}\|_\infty}$ is the induced \mathcal{L}_2 norm of the matrix, equivalently its largest singular value, and n is once again the dimension of the multicule vector.

One may notice that despite our discussion of ε and its components ε_0 , ε_{\min} , and ε_k , the variable ε does not appear in the final bound. This is because the expectation of its contribution to the regret is in fact 0, with small variance on the scale of the state vector lengths we anticipate this algorithm being applied to. A discussion of this and proof of the distributional properties is included in Supplemental Information Section 5.

The sparseness of \mathbf{G} , \mathbf{U} , and others due to the rather tight bounds which biology itself imposes upon the matrices combine to further improve the bound beyond what we show in an asymptotic bound. That is, multicules are in general only directly convertible into a small number of other multicules, and the impacts of other processes not directly modeled can reasonably be assumed to be distributed in a Gaussian fashion by application of the Central Limit Theorem. Additionally, it is reasonable to assume that most aspects of physiology will not change drastically over time on average. As a consequence of these factors, for most \mathbf{A} of interest in this problem, $\|\mathbf{A}\|_1$ and $\|\mathbf{A}\|_\infty$ will likely be $\ll n\delta t$.

The portion of total regret accessible to learning grows as the \sqrt{T} , but this sublinear increase occurs across linear time and so the regret per unit time decays as $\frac{1}{\sqrt{T}}$, meaning that our learning converges. While the unlearnable component of regret grows linearly, it is zero mean and has a variance which converges to zero for large n , yielding an effective overall bound.

Computational Complexity

We show in Section 1 of the Supplemental Information that the time complexity for model evaluation is $\mathcal{O}(qn^2)$, and the number of evaluations per timestep for a given degree of error in terms of integral quadrature sample count is calculated in Section 3 of the SI to be $\varepsilon_k(s) = \mathcal{O}\left(n^2 \exp\left(\frac{-s^2}{n^2}\right)\right)$.

Supposing we want a final error bound of some specific value $\epsilon_f = \inf\{\epsilon_R, \epsilon_\psi\}$, each round defining a new k_0 and requiring assessment across the $\tau - k_0$ planning range, and require a quadrature sample count for each time-step sufficient to reach ϵ_f . We compute the sample number requirement per time step by inverting the asymptotic bound

$$s = \mathcal{O}\left(n \sqrt{\ln\left(\frac{n}{\epsilon_f}\right)}\right)$$

This gives samples per timestep analyzed, and given the $\mathcal{O}(s^3)$ complexity of FWLSBQ the total complexity for error ϵ_f is

⁶See Supplemental Information Section 1 for a discussion of how the linear quadratic model of Ψ can be converted into a single quadratic function.

$$\mathcal{O} = \left(n^6 q^3 \cdot \sqrt[3]{\ln \left(\frac{n}{\epsilon_f} \right)} \right)$$

This bound at first appears concerning given the n^6 term, but because of the practical limitations of experiments we expect n to be on the order of hundreds at most. Additionally, the exponential convergence of FWLSBQ, and the physical limits on a useful ϵ_f imposed by the inevitable level of noise involved in any biological system further diminish the likely computational demands in practice. We know that for each measurement of the system (occurring at intervals of t) we evaluate over the planning range of τ future timesteps. So the asymptotic complexity is then the product of the total operational time T , the planning range length τ , and the quadrature complexity per timestep in planning. Thus the method as a whole has time complexity

$$\mathcal{O} \left(T \frac{\tau}{t} n^6 q^3 \cdot \sqrt[3]{\ln \left(\frac{n}{\epsilon_f} \right)} \right) \quad (12)$$

Given the speed limitations of biological processes, we anticipate the timescales available for computational analysis mean that with appropriate refinement for implementation the bounds should make this approach feasible for near-term application.

DISCUSSION

Thus far there has been relatively little work applying contemporary advancements in control theory and related disciplines to questions of evolutionary systems. There is a recent discussion of the use of dynamic programming for the optimization of cancer therapy,³⁴ however, we have been unable to find any such work beyond that paper. The massive advances in the mathematical study of control systems and artificial intelligence from recent decades have not yet crossed over into the study of evolutionary dynamics and its application to cancer biology. This represents a fertile ground for the use of new tools, the answering of previously unstudied questions, and the framing entirely new questions.

In this paper we expand the theoretical methods available for evolutionary dynamics via integrating contemporary research in control theory and the theory of artificial intelligence. Though a discussion of the experimental component of a practical learning procedure is beyond the scope of this study given it will likely be a contextual decision based on the desired application of directed evolution (clinical, industrial, scientific, etc.), our theoretical analysis stands on its own as a first-of-its kind approach for addressing one of the central questions of applied evolutionary theory. The interoperability of Computational duality makes it particularly suitable for the monitoring and course-correction of evolutionary processes, given the multicules corresponding to an intercellular compartment offer a ready readout for the state of the system provided there are adequately accurate inference methods for translating back and forth with experimental data. Cell sorting and whole-cell mass spectrometry likewise offer a means of reading out the state of intracellular multicules at least below the resolution level of organelles. We expect such inference methods to be very feasible.

We see a number of promising directions for future work, including 1) extending the results to nonlinear transforms $c = \mathbf{B}(x)$ rather than the linear one we assume, 2) analyzing the potential impacts of the difference between the timescale of the respective dynamics of x and u , 3)

tightening the bounds on quadrature estimate by accounting for empirical features of parameter matrices, and of course 4) applying our approach or variants thereof to experimental problems. 366
367

The use of reinforcement learning means that there are minimal requirements of a-priori 368
knowledge of a system. Beyond specifying definitions of multicles and input compounds, we 369
could readily leave all parameter matrices unknown at the start of the problem. This will of course 370
increase the number of trials needed to learn a model when compared with learning given partial 371
prior knowledge of parameters, but the worst-case bounds described here are valid for the cases 372
of any amount of prior knowledge, including the case of no such knowledge. 373

In summary, this study represents three key advancements. First, a novel mathematical 374
formulation of Computational duality for biophysical dynamics which seamlessly links ecology 375
and evolution into a single unified process – just as is the reality in nature. Second, Computational 376
duality’s universality and ability to more richly interface with the mechanistic properties 377
of biosystems has the potential to strengthen the link between theory and experiment in further 378
novel ways. Third, by establishing for the first time the utility of tools from modern artificial 379
intelligence theory cross-applied to the mathematical theory of evolution and the biophysical questions 380
therein, this offers a new explicit link between theoretical biophysics, ecology, evolutionary 381
theory, and artificial intelligence. All three advancements represent interesting directions for future 382
work of a highly interdisciplinary nature. 383

Limitations of the study

384

Because we sought to provide a model that could interact directly with experiments, certain 385
decisions were made which increase the conceptual and computational complexity of the problem. 386
For example, the mathematical model itself is notably more complex than those typically 387
used in evolutionary dynamics. However, each of the modeling decisions was carefully made so 388
that as much prior experimental data as possible could be incorporated into the model before 389
any training might begin. Our goal was to strike a balance between the capacity for integration 390
with physiological experiments – where simpler models have often struggled – and the need 391
to retain a model tractable for algorithmic analysis so that rigorous statements could be made 392
about an interpretable model. Our results on PSRL learning bounds inherently translate to the 393
coarse-grained models typical in evolutionary dynamics, so in a sense that result is incorporated 394
here as the simplest limit case of our work. 395

Ultimately, this paper seeks to be a first step towards incorporating contemporary reinforcement 396
learning with evolutionary dynamics. Significant additional empirical and theoretical work 397
remains, but this provides a foundation for such investigation. 398

Problem Statement

Evolutionary game models are necessarily nonlinear dynamical systems, and in practice at present it is generally only possible to take estimates of their states occasionally due to the need for genetic sequencing or molecular testing of some sort. Thus, any effort to direct evolution will require the application of digital control.^{35,36} In reality, \mathbf{F} is a phenomenological representation of some underlying nonlinear system describing the dynamics of biochemistry and signaling processes within and between biological cells and organisms. Recent improvements in biological data-gathering technology^{37,38} enable the inference of a linear approximation \mathbf{G}_x of an underlying nonlinear system for an n_0 -dimensional vector x of molecular levels within cells. It should be noted that \mathbf{G} will be a sparse matrix, as any given molecule will typically only interact meaningfully with a small number of other molecules. Exceptions absolutely exist, such as the central importance of glucose⁷ and ATP⁸, but by and large \mathbf{G} will be quite sparse.⁹

The complexity of biological systems presents substantial challenges, but this complexity also produces enormous opportunities if methods can be developed for deliberately and precisely controlling them.³⁸⁻⁴⁰ Given there are modeling principles which it is believed should transfer over to complex, data-driven, real-world cases, Model Predictive Control appears to be the most viable option for solving this complex MIMO¹⁰ control problem.^{41,42}

Assuming such a \mathbf{G} as described above, the question will be as follows. Given the ability to modify some comparatively small subset of individual entries of \mathbf{G} in the form $\mathbf{G}_{ij} \rightarrow \hat{\mathbf{G}}_{ij}$ such that $\mathbf{G}_{ij} - \hat{\mathbf{G}}_{ij}$ is sufficiently small for a given application,¹¹ the goal is to develop algorithms for predicting and controlling the evolutionary system. In particular, to make predictions of changes produced by targeted selections of the indices for nonzero $\mathbf{G}_{ij} - \hat{\mathbf{G}}_{ij}$.

This yields the equation

$$d_t c = \mathbf{MC}_a \left(\mathbf{G}_x - \vec{1} c^T (\mathbf{G}_x) \right) \quad (13)$$

where we have in essence simply replaced $\mathbf{F}c$ with \mathbf{G}_x as per the discussion above, and \mathbf{M} is a mapping describing the average rate of mutations converting one cell type into another.

In the context of reinforcement learning, policies are sets of control signals which are input into a system. Given an specific objective and system there will be one or more optimal policies and many sub-optimal ones generally across a spectrum of quality. This objective is termed the "reward" or "value" function, and is defined for a specific problem. Finally, "regret" is used as a metric of the efficacy of some algorithm or approach. Put simply, regret – typically considered as an expectation value – is the difference between the "reward" obtained via a policy and the optimal reward that could have been obtained via a perfect policy.

For the problem of directed evolution, the value function will in general be a function of the various cell types being considered, with more desirable types having increasingly positive (or less negative) contributions to the reward. The vector of these cell types' respective frequencies at time k is represented by $x(k)$. However, experimental supplies are not free, and in a medical

⁷A sugar which serves as the body's main source of energy system-wide.

⁸A high-energy molecule synthesized from a variety of energy sources, which is used to fuel a wide array of cellular processes.

⁹That is, most of the elements of the matrix will be zero.

¹⁰Multiple Input, Multiple Output

¹¹We do not precisely define sufficiently small precisely because we anticipate it could vary significantly from application to application.

context treatments carry with them side effects so an additional term will incorporate their costs. 436
Inputs are represented as $u(k)$. 437

For mathematical tractability, we use a linear reward function which at time k for state x and 438
input u is 439

$$R(x(k), u(k)) = \vec{\omega}^T x(k) - \vec{\mu}^T u(k)$$

Specific $\vec{\omega}$ and $\vec{\mu}$ are determined by the goals in some problem of interest. In this study these 440
goals are set by the humans aiming to control some evolutionary process, but extensions to this 441
model could define it based on an ecology itself to study natural evolution.¹² 442

There are a few options in terms of how to model a system where data is available in the 443
form of values for c , while the dynamics themselves are in truth defined in terms of x . One option 444
is to assume a given estimate of c maps onto an estimated x (and vice versa), and have the 445
model be a hybrid of dynamics over c and x . For the purposes of this study, the approach will 446
be to assume a pseudo-invertable¹³ linear map $Bx = c$ which is time-invariant. Incorporating 447
noise will be relevant later, so we will use the notation $\tilde{B} = Bx + \xi$ with ξ being a vector of zero- 448
mean noise. For the time being, however, we will assume perfect "estimates" and ignore the ξ 449
component of \tilde{B} . Further, we define a vector of inputs to the ecology u , and a matrix Z mapping 450
inputs to multicles. 451

However, it is not in fact required that we have any knowledge of B , G , or any other pa- 452
rameter matrices a priori. This is where the application of reinforcement learning will become 453
central to later sections of the study. For now, we must first define a model of the evolutionary 454
process. The rest of this section will be a discussion of the model and how we can convert it 455
into a Partially Observable Markov Decision Process (POMDP) so as to enable the use of the 456
extensive research in control systems engineering and the theory of artificial intelligence. 457

Computational Duality and Multicles

As mentioned in the introduction, the complexity of evolutionary processes can be enor- 459
mous. Tracking the positions of even a negligible fraction of molecules involved in such pro- 460
cesses is not only infeasible but almost certainly unproductive. However, there is value in being 461
able to capture key features of spatial dynamics as well as more direct biochemical and 462
evolutionary ones. One simplified model which offers a good balance between the two is to analyze 463
the spatial component of a system as a set of discrete partitions. 464

We can imagine attaching to any molecule a hypothetical string of bits to serve as an address 465
of sorts. One value for the bit string could say that it is within a biological cell, another that it 466
is outside the cell. If more fidelity is desired, one could denote intranuclear,¹⁴ cytosolic,¹⁵ or 467
extrecellular. Alternatively (or going further), one could create separate label string values for 468
any given partition of interest, such as one value for the shared space between a group of cells 469
and then additionally one value each for every type of cell as described in the Introduction. 470

In this framework there will in general be no fundamental difference between a molecule 471
moving between partitions vs. being chemically transformed *as it undergoes the same motion*. 472

¹²For instance, one could set $u(k)$ to zero, use a different ecology function than we do here, and have $R(x(k))$ be simply maximization over replication rates. In other words, survival of the fittest.

¹³See Supplemental Information Section 1 for a discussion of the validity of the assumption of pseudo-invertability.

¹⁴That is, within the nucleus of a cell.

¹⁵Within the region between a cell's nucleus and its outer boundary.

That is to say, a process which moves a molecule mol_1 from partition Par_1 to partition Par_2 is
mathematically analogous to another process which took mol_1 and converted it into mol_2 as
it is moved from Par_1 to Par_2 . These two processes are dual to each other, in the sense in
which physicists use the term duality. They are equivalent descriptions of the same underlying
process. The fact that this is not the physical reality of the situation should in general not hamper
its efficacy as a modeling tool, and from an epistemological perspective that is likely all any
duality from physics could claim to be as well.

Using mol_i to denote molecules and Par_j to denote partitions,¹⁶ the equivalence of $\{\text{mol}_1, \text{Par}_1\} \xrightarrow{480} \{\text{mol}_1, \text{Par}_2\} \equiv \{\text{mol}_1, \text{Par}_1\} \rightarrow \{\text{mol}_2, \text{Par}_2\}$ requires introducing language for the relationship
between $\{\text{mol}_1, \text{Par}_2\}$ and $\{\text{mol}_2, \text{Par}_2\}$. We might term these partition-distinguished molecules
particules, but will instead use the term multicules on account of the extensions beyond partitions
as additional properties – and to avoid confusion with the particles of physics. We term the
duality itself Computational duality.

Computational duality allows us to capture richer spatial aspects of evolutionary dynamics
in the molecular reformulation of EGT discussed above, as we can account for molecule placement
simply by creating multiple entries in x which correspond to the same physical molecular
structure across as many partitions as relevant for a given problem. For q cell types of interest,
one extracellular compartment, and n_0 distinct molecular structures of interest, we can have up
to $n_{\max} = n_0(q + 1)$ multicules. It is a set of $n \leq n_{\max}$ multicules which we consider here.

Computational duality is a particularly interesting proposition in that it is capable of converting
essentially any collection of disparate types of biological processes into a single coherent
process type. Abstracting small-molecule structural information and position as part of a collective
state can, in principle, be extended to discretizations of other properties such as conformational
states of proteins, methylation states of DNA. Versions of this concept appear in systems
theory in various contexts, and biophysics allows all properties to be represented as abstract
analogs to molecular structures, and all processes as abstract analogs to chemical reactions.
The general nature of this view is the reason for the term multicule rather than particule. This
combined state space is of course computationally intractably large if one wished to include the
entirety of most given biological processes, but reduced state spaces can always be chosen for
the variables most relevant to a given scientific question. Perhaps even more interesting is that
from a mathematical perspective generalized multicules provide a single, unified framework for
all of biology at the level of molecular and biochemical physiology.

¹⁶With i and j arbitrary indices and not related to any other use of the same index variables elsewhere in the paper

RESOURCE AVAILABILITY

505

Lead contact

506

Requests for further information and resources should be directed to and will be fulfilled by the lead contact, Bryce-Allen Bagley (bbagley@stanford.edu).

507

508

Materials availability

509

No experimental materials are associated with this study.

510

Data and code availability

511

- Because this study focused on the mathematical and algorithmic aspects of an applied theory problem in mathematical biology, no experimental data were used or produced.
- No code was created for this study.
- Likewise, no other resources were generated for this study. The entirety of the work can be found between the paper and the supplemental information.

512

513

514

515

516

ACKNOWLEDGMENTS

517

This work was funded by a research grant from the Stanford University Physician-Scientist Training Program. The study was further supported by grants from the National Institute of Health (17X074, U54CA261717). We would like to thank Mykel Kochenderfer, Arec Jamgochian, and Benjamin van Roy for guidance in literature review and recommendations of relevant papers in the fields of POMDPs and RL, and the former two for helpful feedback on conceptualization in the early stages of the project. We thank Dena Panovska for her thoughtful insights on linking this paper with experimental methods. Additionally, we thank the late Christopher T. Walsh for valuable discussions of underlying concepts in the early stages of the project and for his mentorship. He will be missed.

518

519

520

521

522

523

524

525

526

AUTHOR CONTRIBUTIONS

527

Conceptualization, B.A.B.; methodology, B.A.B.; investigation, B.A.B., N.K.; writing—original draft, B.A.B., N.K.; writing—review & editing, B.A.B. and C.K.P.; funding acquisition, B.A.B. and C.K.P.; resources, B.A.B. and C.K.P.; supervision, C.K.P.

528

529

530

DECLARATION OF INTERESTS

531

We have no competing interests to declare in relation to this paper.

532

SUPPLEMENTAL INFORMATION INDEX

533

1: Derivation of the Evolutionary Dynamics Model. This section contains the intermediate steps between the description of the problem statement and that of the time-evolution operator seen in the body of the paper.	534
	535
	536
2: Model-Predictive Control of the Evolutionary Game. This section describes the Bellman operator and Bellman function, particularly as relates to this paper.	537
	538
3: Reward Function Estimation. This section explains the method for approximating the integral within the Bellman equation, and details the estimation error and computational complexity properties associated with it.	539
	540
	541
4: Derivation of Regret Bounds. This section details the calculation of the regret bound for the application of the PSRL reinforcement learning algorithm to the evolutionary game control problem we study in this paper.	542
	543
	544
5: Statistical Properties of Unlearnable Error ε . This section details the derivation and proof of properties of the component of error which represents a minimum below which the learning algorithm could not improve, including proving that it does not impact the bound on the expectation value of regret.	545
	546
	547
	548
6: A Sketch of an Experimental Protocol. This section gives a rough conceptual description of what an experimental process using our results would consist of, noting that additional work on the algorithms side—beyond the scope of this paper—is needed first.	549
	550
	551

References

552

1. Nowak, M. *Evolutionary Dynamics*. Harvard University Press (2006). 553
2. Rice, S. H. *Evolutionary Theory: Mathematical and Conceptual Foundations*. Sinauer Associates Publishing (2004). 554
3. Basanta, D., and Anderson, A. R. A. (2013). Exploiting ecological principles to better understand cancer progression and treatment. *Interface Focus, The Royal Publishing Society* 3. 555
4. Sandholm, W. H. *Population Games and Evolutionary Dynamics*. MIT Press (2010). 556
5. Cotner, M., Meng, S., Jost, T., Gardner, A., De Santiago, C., and Brock, A. (2023). Integration of quantitative methods and mathematical approaches for the modeling of cancer cell proliferation dynamics. *American Journal of Physiology-Cell Physiology* 324. 557
6. Wölfel, B., te Rietmole, H., Salvioli, M., Kaznatcheev, A., Thuijsman, F., Brown, J. S., Burgering, B., and Staňková, K. (2021). The contribution of evolutionary game theory to understanding and treating cancer. *Dynamic Games and Applications* 12. 558
7. Gatenby, R. A., and Brown, J. S. (2020). Integrating evolutionary dynamics into cancer therapy. *Nature Reviews Clinical Oncology* 17. 559
8. Pucci, C., Martinelli, C., and Ciofani, G. (2019). Innovative approaches for cancer treatment: current perspectives and new challenges. *Ecancermedicalscience*. 560
9. Nikolaou, M., Pavlopoulou, A., Georgakilas, A. G., and Kyrodimos, E. (2018). The challenge of drug resistance in cancer treatment: a current overview. *Clinical & Experimental Metastasis*. 561
10. Tonorezos, E., Devasia, T., Mariotto, A. B., Mollica, M. A., Gallicchio, L., Green, P., Doose, M., Brick, R., Streck, B., Reed, C., and de Moor, J. S. (2024). Prevalence of cancer survivors in the united states. *JNCI: Journal of the National Cancer Institute* 116. 562
11. Delgado-López, P. D., and Corrales-García, E. M. (2016). Survival in glioblastoma: a review on the impact of treatment modalities. *Clinical and Translational Oncology*. 563
12. Tufail, M., Hu, J.-J., Liang, J., He, C.-Y., Wan, W.-D., Huang, Y.-Q., Jiang, C.-H., Wu, H., and Li, N. (2024). Hallmarks of cancer resistance. *iScience* 27. 564
13. McEvoy, J. W. (2009). Evolutionary game theory: lessons and limitations, a cancer perspective. *British Journal of Cancer* 101, 2060–2061. 565
14. Stanková, K., Brown, J. S., Dalton, W. S., and Gatenby, R. A. (2019). Optimizing cancer treatment using game theory. *JAMA Oncology* 5, 96. 566
15. Orlando, P. A., Gatenby, R. A., and Brown, J. S. (2012). Cancer treatment as a game: integrating evolutionary game theory into the optimal control of chemotherapy. *Physical Biology* 9, 065007. 567
16. Packer, M. S., and Liu, D. R. (2015). Methods for the directed evolution of proteins. *Nature Reviews Genetics*. 568

17. Kumar, A., and Singh, S. (2013). Directed evolution: tailoring biocatalysts for industrial 589
applications. *Critical Reviews in Biotechnology*. 590

18. Wang, Y., Xue, P., Cao, M., Yu, T., Lane, S. T., and Zhao, H. (2021). Directed evolution: 591
Methodologies and applications. *Chemical Reviews*. 592

19. Porter, J. L., Rusli, R. A., and Ollis, D. L. (2016). Directed evolution of enzymes for industrial 593
biocatalysis. *ChemBioChem*. 594

20. Lagasse, E., and Levin, M. (2023). Future medicine: from molecular pathways to the col- 595
lective intelligence of the body. *Trends in Molecular Medicine*. 596

21. Krakauer, D., Bertschinger, N., Olbrich, E., Flack, J. C., and Ay, N. (2020). The information 597
theory of individuality. *Theory in Biosciences* 139. 598

22. Osband, I., and Roy, B. V. (2014). Model-based reinforcement learning and the eluder di- 599
mension. *Advances in Neural Information Processing Systems*. 600

23. Osband, I., Russo, D., and Roy, B. V. (2014). (more) efficient reinforcement learning via 601
posterior sampling. *Advances in Neural Information Processing Systems*. 602

24. Traulsen, A., and Glynatsi, N. E. (2023). The future of theoretical evolutionary game theory. 603
Philosophical Transactions of the Royal Society B: Biological Sciences 378. 604

25. May, R. *Stability and Complexity in Model Ecosystems*. Princeton University Press (1973). 605

26. Benner, P., Gugercin, S., and Willcox, K. (2015). A survey of projection-based model reduc- 606
tion methods for parametric dynamical systems. *SIAM Review* 57. 607

27. Feng, L., and Benner, P. (2021). On error estimation for reduced-order modeling of linear 608
non-parametric and parametric systems. *ESAIM: Mathematical Modelling and Numerical 609
Analysis* 55. 610

28. Dogančić, B., and Jokić, M. (2022). Discretization and model reduction error estimation 611
of interconnected dynamical systems. *Proceedings of the 17th IFAC Conference on Pro- 612
grammable Devices and Embedded Systems* 55. 613

29. Nicholson, B., López-Negrete, R., and Biegler, L. T. (2014). On-line state estimation of 614
nonlinear dynamic systems with gross errors. *Computers & Chemical Engineering* 70. 615

30. Zhang, Y., Feng, L., Li, S., and Benner, P. (2015). An efficient output error estimation for 616
model order reduction of parametrized evolution equations. *SIAM Journal on Scientific 617
Computing* 37. 618

31. Chellappa, S., Feng, L., and Benner, P. (2020). Adaptive basis construction and improved 619
error estimation for parametric nonlinear dynamical systems. *International Journal for Nu- 620
merical Methods in Engineering* 121. 621

32. Chellappa, S., Feng, L., and Benner, P. (2024). Accurate error estimation for model reduc- 622
tion of nonlinear dynamical systems via data-enhanced error closure. *Computer Methods 623
in Applied Mechanics and Engineering* 420. 624

33. Russo, D., and Roy, B. V. (2013). Learning to optimize via posterior sampling. *CoRR*. 625

34. Gluzman, M., Scott, J. G., and Vladimirska, A. (2020). Optimizing adaptive cancer therapy: dynamic programming and evolutionary game theory. *Proceedings of the Royal Society B: Biological Sciences* 287. 626
627
628

35. Franklin, G. F., Powell, J. D., and Emami-Naeini, A. *Feedback Control of Dynamic Systems*. Pearson Education (2010). 629
630

36. Franklin, G. F., Powell, J. D., and Workman, M. L. *Digital Control of Dynamic Systems*. Addison-Wesley (1998). 631
632

37. Dillies, M.-A., Rau, A., Aubert, J., Hennequet-Antier, C., Jeanmougin, M., Servant, N., Keime, C., Marot, G., Castel, D., Estelle, J., Guernec, G., Jagla, B., Jouneau, L., Laloë, D., Le Gall, C., Schaëffer, B., Le Crom, S., Guedj, M., and Jaffrézic, F. (2012). A comprehensive evaluation of normalization methods for illumina high-throughput rna sequencing data analysis. *Briefings in Bioinformatics* 14. 633
634
635
636
637

38. Weinberg, R. A. *The Biology of Cancer*. Taylor and Francis (2007). 638

39. Kauffman, S. A. *The Origins of Order: Self-Organization and Selection in Evolution*. Oxford University Press (1993). 639
640

40. Krakauer, D. C., ed. *Worlds Hidden in Plain Sight*. Santa Fe Institute Press (2019). 641

41. Rawlings, J. B., Mayne, D. Q., and Diehl, M. M. *Model Predictive Control: Theory, Computation, and Design*. Nob Hill Publishing (2017). 642
643

42. Grune, L., and Pannek, J. *Nonlinear Model Predictive Control: Theory and Algorithms*. Springer (2011). 644
645

43. Briol, F.-X., Oates, C. J., Girolami, M., and Osborne, M. A. (2015). Frank-wolfe bayesian quadrature: Probabilistic integration with theoretical guarantees. *Advances in Neural Information Processing Systems*. 646
647
648

44. Kanagawa, M., and Hennig, P. (2019). Convergence guarantees for adaptive bayesian quadrature methods. *Advances in Neural Information Processing Systems*. 649
650

45. Osborne, M. A., Duvenaud, D., Garnett, R., Rasmussen, C. E., Roberts, S. J., and Ghahramani, Z. (2012). Active learning of model evidence using bayesian quadrature. *Advances in Neural Information Processing Systems*. 651
652
653

46. Lacoste-Julien, S., Lindsten, F., and Bach, F. (2015). Sequential kernel herding: Frank-wolfe optimization for particle filtering. *Journal of Machine Learning Research*. 654
655

47. Strens, M. (2000). A bayesian framework for reinforcement learning. *Advances in Neural Information Processing Systems*. 656
657

48. Dubuc, B., Quiniou, J. F., Roques-Carmes, C., Tricot, C., and Zucker, S. W. (1989). Evaluating the fractal dimension of profiles. *Phys. Rev. A* 39. 658
659

49. Mandelbrot, B. B., and Mandelbrot, B. B. *The fractal geometry of nature* vol. 1. WH freeman New York (1982). 660
661

50. Tricot, C. *Curves and fractal dimension*. Springer Science & Business Media (1994). 662

Supplemental Information 1: Derivation of the Evolutionary Dynamics Model

663

664

System of 1st Order Matrix Differential Equations

665

$$d_t c_i = c_i \left(\left(\sum_j \mathbf{F}_{ij} c_j \right) - c^T \mathbf{F} c \right)$$

as a description for a given type. Extending to all types present, we have

666

$$d_t c = \mathbf{C}_a \left(\mathbf{F} c - \vec{1} c^T \mathbf{F} c \right) \quad (14)$$

Here \mathbf{C}_a is a diagonal matrix whose entries are the elements of c , defined explicitly as

667

$$\mathbf{C}_a = \sum_{i=1}^q \mathbf{E}_i c^T \vec{e}_i \quad (15)$$

Where here \vec{e}_i is the vector with all zero entries save for a 1 at entry i , and \mathbf{E}_i is the $q \times q$ matrix with the q -th diagonal as 1 and all other entries as 0. We have subscripted this matrix \mathbf{C}_a for convenience and cleaner notation in certain more complex calculations to come.

668

669

670

With the parameter matrices \mathbf{M} , \mathbf{B} , \mathbf{C}_B , and \mathbf{G} defined as in the Results section, we proceed through the derivation of the model as respectively a 1st-order system of equations and a single 2nd-order equation. As a reminder, $\mathbf{M} \in \mathbb{R}^{q \times q}$, $\mathbf{C}_B \in \mathbb{R}^{q \times q}$, $\mathbf{B} \in \mathbb{R}^{q \times n}$, $\mathbf{G} \in \mathbb{R}^{q \times n}$, and $\mathbf{Z} \in \mathbb{R}^{q \times m}$

671

672

673

$$d_t c = \mathbf{M} \mathbf{C}_B^T \left(\mathbf{G} x - \vec{1} (\mathbf{B} x)^T (\mathbf{G} x) \right) + \mathbf{Z} u \quad (16)$$

$$d_t c = \mathbf{C}_B \left(\mathbf{M}^T \mathbf{G} x - \mathbf{M}^T \vec{1} (\mathbf{B} x)^T (\mathbf{G} x) \right) + \mathbf{Z} u$$

Here we will assume that \mathbf{M} is symmetric, which is in general very close to the empirical truth. Additionally each row of \mathbf{M} sums to 1, so $\mathbf{M} \vec{1} = \vec{1}$. Additionally, \mathbf{C}_B is defined as

674

675

$$\mathbf{C}_B = \sum_{i=1}^q \mathbf{E}_i ((\mathbf{B} x)^T \vec{e}_i) \quad (17)$$

In this study \mathbf{E}_i is defined as the matrix where $E_{jk} = 0$ in all cases except where $j = k = i$, where it is 1. That is, the matrix of all zeros except for a 1 at the i -th diagonal entry. Thus, the above is equivalently

676

677

678

$$d_t c = \mathbf{C}_B \left(\mathbf{M} \mathbf{G} x - \vec{1} (\mathbf{B} x)^T (\mathbf{G} x) \right) + \mathbf{Z} u$$

as the simplified model for the dynamics of c . Completing the conversion by our earlier definition that $c = \mathbf{B} x$ is a time-invariant mapping, if we define \mathbf{B}^{-1} as a Moore-Penrose left pseudoinverse of \mathbf{B} , we know that $\mathbf{B}^{-1} d_t c = d_t x$. Of note, computing this pseudoinverse is equivalent to SVD, and thus has a time complexity of $\mathcal{O}(qn^2)$. However, this is a one-time cost. Because

679

680

681

682

we are claiming a left pseudoinverse, \mathbf{B} must have linearly independent columns. Since each column corresponds to one multicule, this is almost certainly true in general because the selected multicules for a model will not include all actual multicules in the system. \mathbf{B} thus encodes interactions with what could be thought of as "implicit" multicules, and with sufficiently precise measurement the columns of \mathbf{B} are very unlikely to be linearly dependent for cell/environment types (elements of c) of interest. In other words, the two types would need to be so similar with respect to their actions on molecules as to be difficult to distinguish via experiment, and could thus reasonably be considered one type for practical purposes. Intuitively, many mutations do not modify molecular processes. An alternate way of framing this relies less on how types are distinguished, and instead simply saying that if two multicules behave identically with respect to \mathbf{B} – equivalent to saying their columns are linearly dependent – then we will simply approximate them as the same multicule and modify other parameter matrices in the model correspondingly.

Noting that $\mathbf{C}_B \vec{1} = c = \mathbf{B}x$ and progressing through the derivation

$$d_t x = \mathbf{B}^{-1} \mathbf{C}_B \left(\mathbf{M} - \vec{1}(\mathbf{B}x)^T \right) \mathbf{G}x + \mathbf{B}^{-1} \mathbf{Z}u$$

$$d_t x = \mathbf{B}^{-1} \mathbf{C}_B \left(\mathbf{M}\mathbf{G}x - \vec{1}(x^T \mathbf{B}^T \mathbf{G}x) \right) + \mathbf{B}^{-1} \mathbf{Z}u \quad (18)$$

However, because treatments – the input signals of interest – are not maintained at a constant and level dose over time, we must account for the dynamics of \mathbf{G} . This is equivalent to the dynamics of a matrix $\Delta \mathbf{U} \mathbf{V}$ as discussed earlier. Because we want the dynamics of \mathbf{G} to deviate from some baseline in proportion with drug concentrations (themselves approximately exponentially decaying after a dose is administered), the functional form should be roughly

$$\mathbf{G}(t) = \mathbf{G}_0 + \Delta \mathbf{U} \mathbf{V} \quad (19)$$

With \mathbf{U} the matrix defined as the decay from a baseline $\tilde{\mathbf{U}}$, a matrix of inputs (chemical or otherwise) into the system which is itself defined as

$$\tilde{\mathbf{U}} = \sum_{i=1}^m \mathbf{E}_i u(\tilde{t})^T \vec{e}_i \quad (20)$$

Here \mathbf{E}_i and \vec{e}_i are used just as with the definition of \mathbf{C}_B in Equation (17). To clarify dimensions, $m = m$, $\mathbf{U} \in \mathbb{R}^{m \times m}$, $\Delta \in \mathbb{R}^{q \times m}$, and $\mathbf{V} \in \mathbb{R}^{m \times n}$. Defining $u(\tilde{t})$ is the magnitude of the dose applied at the last treatment, which occurred at time \tilde{t} . For simplicity of notation, in this derivation t will be shifted such that

The diagonals will themselves be very sparse, since a patient is unlikely to be treated with more than a very small number of medications at most at any given time. The matrix Δ is then the degree to which each drug (signal) would effect the column of \mathbf{G} with which it interferes, depending on which type within c that row of \mathbf{G} corresponds to. It is thus a representation of the susceptibilities to different forms of interference. In situations where more than one drug targets a given column of \mathbf{G} , separate Δ matrices may be defined and summed. The equation would not be changed in any significant sense by this. While more complex functional forms may describe the amount of drug in a disease microenvironment at a given time (termed "bioavailability"), for the purposes of this analysis the nonzero inputs may be treated as impulses followed by exponential decays. A separate exponential parameter Ξ_i will be associated with each decay. Thus, it's equivalent to write Equation (19) as

$$\mathbf{G}(t) = \mathbf{G}_0 + \Delta \tilde{\mathbf{U}} e^{-\Xi t} \mathbf{V} \quad (21)$$

We have chosen to represent Ξ as a diagonal matrix having positive entries simply for clarity's sake, as multiplying it by -1 is a visual reminder that this is a decay process. 718
719

$$d_t \mathbf{G} = -\Delta \tilde{\mathbf{U}} \Xi e^{-\Xi t} \mathbf{V} \quad (22)$$

These results provide the full model of Equation (8). 720

It is important to note three key aspects of this model which may not be superficially clear. 721
As mentioned in the Results subsection Dynamical System Model for Multicule Evolutionary Dy- 722
namics, the $\vec{1}x^T \mathbf{B}^T \mathbf{G}x$ term can be represented by an additional "bookkeeping" variable in the 723
system of equations. This preserves the model's quadratic structure, which is necessary for the 724
proofs of regret bounds. When it comes to the other three aspects just referenced, first, the 725
summation within \mathbf{C}_B means that the first equation of the 2-equation system is a summation 726
over a collection of quadratic models. Second, By concatenating x and u and replacing the 727
relevant matrices with larger combined matrices including the terms corresponding to each original 728
matrix, we can make clearer the quadratic structure. However, this is not at all illustrative, so the 729
model is presented as above (and below, for the single 2nd-order equation). Third and finally, 730
while inferring the matrices Δ , \mathbf{V} , and Ξ is a time-invariant problem, it can also be defined in 731
terms of another "bookkeeping" variable. Specifically, this second "bookkeeping" variable would 732
be defined the time since last input impulse¹⁷ and the model would remain quadratic by inferring 733
the 2nd-order Taylor series of $\Delta \mathbf{U} e^{-\Xi t} \mathbf{V}$ and $\Delta \Xi \mathbf{U} e^{-\Xi t} \mathbf{V}$ instead of the exact functions – again 734
using the concatenation procedure noted above. 735

Single 2nd Order Matrix Differential Equation

736

For the purposes of our approach, it is helpful to restate the model as a single, 2nd order 737
equation. 738

$$d_t^2 x = d_t \mathbf{B}^{-1} \mathbf{C}_B (\mathbf{M}(\mathbf{G}_0 + \Delta \tilde{\mathbf{U}} e^{-\Xi t} \mathbf{V})x) - d_t \mathbf{B}^{-1} \mathbf{C}_B \vec{1}(x^T \mathbf{B}^T (\mathbf{G}_0 + \Delta \tilde{\mathbf{U}} e^{-\Xi t} \mathbf{V})x) + \mathbf{B}^{-1} \mathbf{Z} d_t u$$

From here we can derive the single-equation form of the model. 739

$$\begin{aligned} d_t^2 x = & \mathbf{B}^{-1} \frac{d \mathbf{C}_B}{d_t} \left(\mathbf{M} - \vec{1}x^T \mathbf{B}^T \right) (\mathbf{G}_0 + \Delta \tilde{\mathbf{U}} e^{-\Xi t} \mathbf{V})x \\ & + \mathbf{B}^{-1} \mathbf{C}_B \left[\mathbf{M} \left(\mathbf{G}_0 \frac{dx}{dt} + \Delta \tilde{\mathbf{U}} e^{-\Xi t} \left(\mathbf{V} \frac{dx}{dt} - \Xi \mathbf{V} x \right) \right) \right. \\ & \left. - \vec{1}x^T \mathbf{B}^T \left(2 \mathbf{G}_0 \frac{dx}{dt} + \Delta \tilde{\mathbf{U}} e^{-\Xi t} \left(2 \mathbf{V} \frac{dx}{dt} - \Xi \mathbf{V} x \right) \right) \right] + \mathbf{B}^{-1} \mathbf{Z} d_t u \end{aligned}$$

If we wish to clean it up further for aesthetic purposes, or for clarity in the sort of computational complexity analysis on which this study focuses, we can ignore certain constant factors to 740
get the cleaner form. 741
742

¹⁷ $t - \bar{t}$, as discussed below in the subsection on System Stability.

$$d_{t^2}^2 x = \mathbf{B}^{-1} \frac{d\mathbf{C}_B}{dt} \left(\mathbf{M} - \vec{1} x^T \mathbf{B}^T \right) (\mathbf{G}_0 + \Delta \tilde{\mathbf{U}} e^{-\Xi t} \mathbf{V}) x \\ + \mathbf{B}^{-1} \mathbf{C}_B \left[\left(\mathbf{M} - \vec{1} x^T \mathbf{B}^T \right) \left(\mathbf{G}_0 \frac{dx}{dt} + \Delta \tilde{\mathbf{U}} e^{-\Xi t} \left(\mathbf{V} \frac{dx}{dt} - \Xi \mathbf{V} x \right) \right) \right] + \mathbf{B}^{-1} \mathbf{Z} d_t u$$

Computational Complexity of Model Evaluation

743

A quick calculation will show the time complexity of evaluating the model. Here we assume trivial algorithms for matrix multiplication, but of course they can be replaced with more efficient algorithms if the dimensions of x and c are sufficiently large to justify it. Recalling again that $\mathbf{C}_B, \mathbf{M} \in \mathbb{R}^{q \times q}$, $\mathbf{B}^{-1} \in \mathbb{R}^{n \times q}$, $\mathbf{G}_0 \in \mathbb{R}^{q \times n}$, $\Delta, \mathbf{Z} \in \mathbb{R}^{q \times m}$, $\tilde{\mathbf{U}}, \Xi \in \mathbb{R}^{m \times m}$, and $\mathbf{V} \in \mathbb{R}^{m \times n}$ we assess evaluating

744

745

746

747

748

$$d_{t^2}^2 x = \mathbf{B}^{-1} \frac{d\mathbf{C}_B}{dt} \left(\mathbf{M} - \vec{1} x^T \mathbf{B}^T \right) (\mathbf{G}_0 + \Delta \tilde{\mathbf{U}} e^{-\Xi t} \mathbf{V}) x \\ + \mathbf{B}^{-1} \mathbf{C}_B \left[\left(\mathbf{M} - \vec{1} x^T \mathbf{B}^T \right) \left(\mathbf{G}_0 \frac{dx}{dt} + \Delta \tilde{\mathbf{U}} e^{-\Xi t} \left(\mathbf{V} \frac{dx}{dt} - \Xi \mathbf{V} x \right) \right) \right] + \mathbf{B}^{-1} \mathbf{Z} d_t u$$

In terms of computational complexity, the dominant term in the above equation is (separated out) $x^T \mathbf{B}^T \Delta \tilde{\mathbf{U}} e^{-\Xi t} \Xi \mathbf{V} x$ because of the fact that the superficially largest term $\mathbf{B}^{-1} \mathbf{C}_B \vec{1} x^T \mathbf{B}^T \Delta \tilde{\mathbf{U}} e^{-\Xi t} \Xi \mathbf{V} x$ is reduced by being a vector multiplication with $\vec{1}$ multiplied by some scalar value. Evaluating this term has complexity $\mathcal{O}(n^2)$, which is what we would expect for a quadratic model with state vector of length n and input vector of length $m \ll n$. In the conservative case where we account for \mathbf{C}_B being a linear sum to provide an exactly quadratic model, we will sum over q terms such that we have evaluation complexity $\mathcal{O}(qn^2)$.

749

750

751

752

753

754

755

System Stability

756

In the standard EGT model

757

$$d_t c_i = c_i \left(\left(\sum_j \mathbf{F}_{ij} c_j \right) - c^T \mathbf{F} c \right)$$

represents the dynamics of one type, and

758

$$d_t c = \mathbf{C}_a \left(\mathbf{F} c - \vec{1} c^T \mathbf{F} c \right) \quad (23)$$

for a collection of types. As before, \mathbf{C}_a is a diagonal matrix whose entries are the elements of c , defined explicitly as

759

760

$$\mathbf{C}_a = \sum_{i=1}^q \mathbf{E}_i c^T \vec{e}_i \quad (24)$$

Where here \vec{e}_i is the vector with all zero entries save for a 1 at entry i , and \mathbf{E}_i is the $q \times q$ matrix with the q -th diagonal as 1 and all other entries as 0. We have subscripted this matrix \mathbf{C}_a for convenience and cleaner notation in certain more complex calculations to come. 761
762
763

In this model, $\sum_i c_i = 1$ bounds the state space, which is made valid by the c_i being interpreted as being the fraction of a total population currently comprised of the i -th type. Summing over all types thus yields 1. This preserves stability in the deterministic case, but is known (and can readily be shown) to be unstable in the stochastic case in the limit as $t \rightarrow \infty$. Discussions of this can be found in standard textbooks on EGT.^{1,4} It also holds if a Markov matrix \mathbf{M} is included to model mutations between types. As discussed elsewhere, such an \mathbf{M} will be a small deviation from the identity matrix, and can to first order be assumed to take on a form where the off-diagonal entries are some small positive number ϵ and the diagonal entries $1 - (q - 1)\epsilon$. Of note, this is not the ϵ error term used elsewhere in this study, and in this paragraph we are merely using the standard notation in analysis for a small value. 764
765
766
767
768
769
770
771
772
773

However, even in a deterministic case with an idealized x containing all multicles (and thus molecules) in the system, and a perfect \mathbf{G} and \mathbf{B} to exactly map $x \rightarrow c$, stability would not be preserved. This is because \mathbf{G} and \mathbf{B} are *statistical mappings* – inferences about the relationship between relevant aspects of genotype, phenotype, and other experimental measures of an evolutionary system. At a physical level, it is also the case that biochemical processes do not preserve the material in the system – if nothing else in the sense of releasing gasses and producing unusable byproducts. We are thus interested in being able to say some things about the stability of our biophysical cybernetics approach. 774
775
776
777
778
779
780
781

$$d_t x = \mathbf{B}^{-1} \mathbf{C}_B \left(\mathbf{M} \mathbf{G} x - \vec{1} (x^T \mathbf{B}^T \mathbf{G} x) \right) + \mathbf{B}^{-1} \mathbf{Z} u \quad (25)$$

Here the issue of instability can be resolved by recognizing it is exactly the sort of imprecision control theory must always account for. Measurements of some components of x are our partial observation just as would be the case in any POMDP, and more broadly most control systems. Thus the control signal u can be used to respond to readouts in the same general fashion as any robust model-predictive control system for any application. This is in some sense inevitable, as there must be external input of material and energy for a system to persist, and similarly there is loss of material as waste. Entropy is a harsh taskmaster. 782
783
784
785
786
787
788
789

However, allowing the inputs to alter the dynamical system itself, in the form of u having effects on \mathbf{G} in addition to the more direct effects on x , further complicates the situation. 789
790

Our complete model 791

$$\begin{aligned} d_{t^2}^2 x = & \mathbf{B}^{-1} \frac{d \mathbf{C}_B}{d_t} \left(\mathbf{M} - \vec{1} x^T \mathbf{B}^T \right) (\mathbf{G}_0 + \Delta \tilde{\mathbf{U}} e^{-\Xi t} \mathbf{V}) x \\ & + \mathbf{B}^{-1} \mathbf{C}_B \left[\left(\mathbf{M} - \vec{1} x^T \mathbf{B}^T \right) \left(\mathbf{G}_0 \frac{dx}{dt} + \Delta \tilde{\mathbf{U}} e^{-\Xi t} \left(\mathbf{V} \frac{dx}{dt} - \Xi \mathbf{V} x \right) \right) \right] + \mathbf{B}^{-1} \mathbf{Z} d_t u \end{aligned}$$

Using the previously stated assumption that u – and thus \mathbf{U} – are the result of impulse inputs followed by a decay back to some baseline $\mathbf{G} = \mathbf{G}_0$ and $u = 0$, we have a clean functional form of 792
793
794

$$u_j(t - \bar{t}) = \tilde{u}_j(\bar{t}) e^{-\Xi_{j,j}(t - \bar{t})} \quad (26)$$

Here \bar{t} is the time of the last impulse input. Since Ξ is a diagonal matrix, $e^{-\Xi t}$ is also diagonal. Discretizing over time, $\Delta \tilde{\mathbf{U}} \Xi e^{-\Xi t} \mathbf{V}$ – and $\Delta \tilde{\mathbf{U}} e^{-\Xi t} \mathbf{V}$ similarly – would represent a set of matrices, one for each of the k steps of width δt . One could in principle run PSRL²² with the goal of learning each such matrix and increasing the asymptotic complexity by a factor defined by the number of timesteps beyond which any further decay dynamics is irrelevant. However, they are all the same function of $t - \bar{t}$, so this would be redundant from a learning perspective.

This ultimately reduces the dynamic nature of \mathbf{G} to a series of time-dependent functions of $t - \bar{t}$. While the regret bounds offered by PSRL assume time-invariant matrices, the the simple nature of the functional form we assume makes the mapping to a time-invariant model trivial in the periods between impulse inputs. One can imagine functional forms for $\mathbf{G}(t)$ complex enough to warrant that sort of piece-wise learning, which would scale up the time complexity of the learning process by a factor of the average time span between inputs, as defined according to a given timescale of discretization.

Supplemental Information 2: Model Predictive Control of the Evolutionary Game

This is a nonlinear dynamical system just as with Equation (1), and in the next section we proceed to a discussion of how model predictive control can be used to influence it. Finally, for the sake of our later analysis, it can be useful to convert the system in Equation (8) into a single, equivalent higher-order equation. The derivation is somewhat messy, so they can be found in Section 1 of the Supplemental Information as well. Recalling our earlier mention of a "bookkeeping" variable, we note that it is not illustrative in the context of the model's dynamics, but does verify the model's property of being a quadratic dynamical system. That property will be important later, as regret bounds for model-predictive reinforcement learning are not known for all but a small number of very specific equations and a much smaller number of model classes – linear, quadratic, and generalized linear models being the only such general classes for which there are to our knowledge adequate bounds.

To condense our notation for the proceeding sections, we will discretize the 2nd-order dynamical model into a Markov Decision Process (MDP) transfer function.

$$\Psi(x'|x, u) = \psi(x, u) + \vec{\xi}(x_{k+1} - x_k) \cdot (\delta t) = \frac{d^2x}{dt^2}(\delta t)^2 + \vec{\xi}(x_{k+1} - x_k) \cdot (\delta t) \quad (27)$$

with $\vec{\xi}$ a zero-mean sub-Gaussian noise vector to account for model error (and absorbing the earlier ξ term), multiplied by (δt) so that it is proportional to the time-step length. There is thus a parameter σ_ψ describing the maximum variance across entries of this sub-Gaussian noise vector. The noise is sub-Gaussian rather than Gaussian to prevent the mathematical difficulties connected with the MDP RL analysis on an unbounded range of outcomes, and this is also physically correct given conservation of mass. Because we can only observe a subset of the system's components at any given time, this MDP is termed "Partially Observable" and is thus a POMDP.

As we will soon show, the use of reinforcement learning means that there are minimal requirements of a-priori knowledge of a system. Beyond specifying definitions of multicles and input compounds, we can leave all parameter matrices unknown at the start of the problem. this will of course increase the number of trials needed to learn a model when compared with learning given partial prior knowledge of parameters, but the worst-case bounds described in the Results subsection on Parameter Learning are valid for the cases of any amount of prior knowledge, including the case of no such knowledge. Armed with this single-equation POMDP, we proceed to develop the optimal control results.

For the finite horizon discrete case, which will be used here for both theoretical and practical reasons, we have the following reward function. With $R(x(t), u(t))$ the instantaneous reward function of a given state $x(t)$ and input $u(t)$ at time t , and $L(x(t_f))$ the reward associated with the state at the end of the time horizon considered, the reward of some control sequence $u(t_i \rightarrow t_f)$ is

$$V(t_i, x(t_i), u(t_i \rightarrow t_f)) = L(x(t_f)) + \sum_{t_i}^{t_f} dt R(x(t), u(t), t) \quad (28)$$

While the functional form of $L(\cdot, \cdot)$ could be defined differently for various applications, here

we assume there are relative values which correspond to each cell type in an ecological setting.¹⁸ These values form a vector which maps from multicule state to the value function. A similar vector maps input chemicals to their associated costs, and we concatenate these vectors into $\vec{\omega}$. We must also constrain $u(k)$ in order to prevent nonsense solutions, as is it mathematically possible but in practice impossible to over-specify the control of every single molecular detail of a system. However, a conservative scalar weight will serve the same purpose. We define $L(\cdot)$ and $R(\cdot, \cdot)$ with corresponding constraints as:

$$L(x(t_f)) = \vec{\nu}^T \{x(t_f), 0, \dots, 0\} \quad (29)$$

$$R(x(k), u(k)) = \vec{\omega}^T \{x(k), u(k)\} \quad (30a)$$

$$\|u(k)\|_2 \leq \theta \quad (30b)$$

Here we are using $\{x(k), u(k)\}$ to denote the concatenation of the two vectors, and $\{x(t_f), 0, \dots, 0\}$ a vector of equal length with all dimensions normally corresponding to $u(k)$ set to zero. The rewards associated with different cell types are defined by the non-zero entries of $\vec{\nu}$ and $\vec{\omega}$. Using L_2 to constrain more intense input concentrations and prevent paths which would require unreasonable control inputs, we threshold with respect to θ . This is convenient for incorporation with the analysis of²², but in principle could take on a different functional form. The inputs will presumably be subtracted from the reward function simply on the basis that they will not be free in experimental settings.

In practice we anticipate that $\vec{\nu}$ and $\vec{\omega}$ will be the same, and this is assumed in our analysis. $R(\cdot, \cdot)$ will be associated with a single sub-Gaussian variance σ_R , which will be relevant to the derivation of our regret bounds later.

Additionally, in the general case $\vec{\omega}$ will not be known exactly in advance, and so a mapping must be learned. To clarify this, one can imagine there being a known $\vec{\omega}'$ which is specified for a given problem, but there is some unknown transform which we can approximate as Υ such that $\vec{\omega} \approx \Upsilon \vec{\omega}'$. Of course $\Upsilon \vec{\omega}'$ is itself a vector, so we use its approximation $\vec{\omega}$. If all entries of $\vec{\omega}$ are considered to be known exactly for a specific case, then the terms corresponding to $R(\cdot, \cdot)$ can be removed from the regret bounds derived later.

Discretizing over time, we would like to frame the problem in the form of a Bellman equation,

$$V(x(k), u(k)) = L(x(\tau), u(\tau)) + \gamma \int_X dx \Psi(x(k+1)|x(k), u(k)) V(x(k+1), u(k+1)) \quad (31)$$

With $V(\cdot, \cdot)$ the reward of a given state and γ a discount factor,¹⁹ our optimal input strategy (in controls and AI terms, the "policy") is given by the following, subject to ceasing to evaluate beyond a chosen time-horizon τ .

$$u^* = \arg \max_{u(\cdot)} V(x(k_0), u(k_0)) \quad (32)$$

Which evaluates from some time k_0 until the planning horizon τ . Here we do not make any assumptions about the relationship between the interval \underline{t} between noisy observations of the

¹⁸Bearing in mind that this is simply the most general phrasing. Any evolutionary system from tumors to directed evolution for chemical manufacturing each have their own ecology.

¹⁹A scaling parameter which prioritizes events closer in the future over those further on.

state and the planning interval τ . This may be disregarded in terms of our proofs of bounds, 875
because observations between k_0 and τ will only improve our knowledge beyond the worst case 876
of only one observation each round at k_0 itself. 877

Supplemental Information 3: Reward Function Estimation

878

Franke-Wolfe Bayesian Quadrature

879

Bayesian Quadrature is a well-established collection of methods for computing numerical solutions to probabilistic integrals.^{43–45}

880

881

The Franke-Wolfe algorithm has recently been applied to some problems in statistical learning, such as particle filtering⁴⁶ and Bayesian Quadrature⁴³. In contrast with the Supplemental Information section Derivation of Regret Bounds Below, we will not discuss the definitions and derivations from⁴³ at any noteworthy length, as transferring their results to this case is somewhat more straightforward.

882

883

884

885

886

In essence, Franke-Wolfe Bayesian Quadrature (FWBQ) and its more accurate cousin Franke-Wolfe Line Search Bayesian Quadrature (FWLSBQ) use the Franke-Wolfe algorithm to optimize over a convex hull of the posterior distribution volumes to which a given prior could map. This enables a discrete integral of the form $\int_{a \in \mathcal{A}} p(a) f(a) da$ to be solved with accuracy converging faster than other quadrature methods, with respect to number of regions a_i sampled for the discretization.

887

888

889

890

891

892

Calculations

893

At each step, we want to solve for

894

$$\int_{x_{k+1} \in X} \Psi(x_{k+1} | x_k, u_k) V(x_{k+1}, u_{k+1}) = \int_{x_{k+1} \in X} \left(\psi(x_k, u_k) + \vec{\xi} \cdot (\delta t) \right) V(x_{k+1}, u_{k+1})$$

But since $\psi(x_k, u_k)$ and δt are constant and the noise is additive,

895

$$V(\psi(x_k, u_k), u_{k+1}) + \int_{x_{k+1} \in X} \left(\vec{\xi} \cdot (\delta t) \right) V(x_{k+1}, u_{k+1})$$

is equivalent to separating the integral into deterministic and stochastic components

896

$$V(\psi(x_k, u_k), u_{k+1}) + (\delta t) \int_{x_{k+1} \in X} \vec{\xi}(x_{k+1} - x_k) V(x_{k+1}, u_{k+1})$$

As noted earlier, with variance on the sub-Gaussian noise σ_ψ in the transition process

897

898

$$\vec{\xi}(x_{k+1} - x_k) = \frac{1}{\sqrt{2\pi\sigma_\psi}} e^{-(x_{k+1} - x_k)/(2\sigma_\psi)} \quad (33)$$

899

900

901

902

903

we can make use of the distribution's properties to cut down on the number of voxels which must be sampled for a given level of accuracy. σ may be small enough that we need only sample a section of the space, accepting that the accuracy bounds of FWLSBQ will be multiplicatively limited by the bounds from cutting off after a certain number of σ . This is readily accomplished by mandating that all voxels considered must be within some Euclidean distance proportional to σ . That is, all voxels in $k + 1$ for which $\|x_{k+1} - x_k\|_2 \leq \kappa(\delta t)\sqrt{\sigma_\psi}$ with κ a tuning parameter and

(δt) included so the parameter need not scale with the timestep size. This helps to reduce the effective sample count s which is needed, reducing the run-time per integration to be performed. 904
905

Because the state space is the unit $\mathcal{O}(n)$ -cube, is its diameter just 1, and with s samples the side-length of each voxel is $\frac{1}{\sqrt[n]{s}}$. Thus, we have a polytope diameter of $D = \frac{n}{\sqrt[n]{s}}$ for the n-volume. 906
907

Next, R is the radius of the smallest n -sphere which will contain our post-transition state space. Specifically, $R = \frac{\sqrt[n]{s}}{2}$, because we need to account for the full region of the state space 908
909 across which the system could move from one specific time-step to another. 910

FWLSBQ has time complexity bounded by $\mathcal{O}(s^3)$ in the number of points sampled, but the 911
approximation error also converges as 912

$$\text{err}_{\text{approx}}(s) = \mathcal{O} \left(\frac{n^2}{\sqrt[n]{s}} \exp \left(\frac{-s^2}{n^2 / (\sqrt[n]{s})^2} \right) \right)$$

Since n will be on the order of hundreds, $\sqrt[n]{s} \approx 1$ for any computationally feasible value of s . 913
So the approximation error bound effectively simplifies to 914

$$\text{err}_{\text{approx}}(s) = \mathcal{O} \left(n^2 \exp \left(\frac{-s^2}{n^2} \right) \right)$$

While at $\mathcal{O}(s^3)$ – with s the number of samples used to compute the integral – it is more 915
computationally expensive than other existing quadrature algorithms, FWLSBQ provides exponentially 916
faster accuracy convergence in the number of samples. For a state space of dimension 917
 n ,²⁰ the convergence of the error between the true integral T_f and the estimate E_f goes as 918

$$\varepsilon_k(s) = \text{err}_{\text{approx}}(s) = \mathcal{O} \left(n^2 \exp \left(\frac{-s^2}{n^2} \right) \right) \quad (34)$$

Evaluation of the model requires $\mathcal{O}(qn^2)$ in terms of the dimensions of the state, observable, 919
and input vectors, and this is shown briefly in Supplemental Information Section 1’s subsection 920
on Computational Complexity of Model Evaluation. This is then the time complexity for each 921
sample in a given timestep’s quadrature. It is worth noting, however, that because the parameter 922
matrices should in general be sparse,²¹ this upper bound is a decidedly conservative one. 923

²⁰Recalling that n is the cardinality of x .

²¹This sparseness is anticipated simply via the fact that most molecules involved in an organism’s physiology have substantive interactions with only a small proportion of all other relevant molecules.

Supplemental Information 4: Derivation of Regret Bounds

924

In this section, properties of this problem are derived and/or proven (as the case may be) to prove regret bounds for the use of the Posterior Sampling Reinforcement Learning (PSRL) algorithm described in^{22,23,47}. We will make particular use of the results from²², which

925

926

927

Minkowski-Bouligand Dimension and Lipschitz Continuity

928

The covering number for balls of radius α is $N_\alpha^{cov} \leq \left(\frac{2k\sqrt{d}}{\alpha}\right)^d$ with maximum norm k and dimension d . Since we are interested in the norms of the matrices \mathbf{B} , \mathbf{G} , $\mathbf{\Xi}$, $\mathbf{\Delta}$, and \mathbf{V} we must instead use a matrix norm. Thankfully, there are equivalence relations which connect most categories of matrix norms, and the induced Euclidean norm of some matrix \mathbf{A} is bounded from above as $\|\mathbf{A}\|_2 \leq \sqrt{\|\mathbf{A}\|_1\|\mathbf{A}\|_\infty}$ by special case of Holder's inequality. For matrix norms, $\|\mathbf{A}\|_1$ and $\|\mathbf{A}\|_\infty$ have different definitions than their vector counterparts. The former is the maximum column-wise absolute sum, and the latter the maximum row-wise absolute sum. In other words, the maximum L_1 norm over columns and rows, respectively. Given we can reasonably expect $m < q \ll n$, the largest of our matrices will have $n \cdot q$ terms in the cases of \mathbf{B} and \mathbf{G} , these are the dimensions which will dominate asymptotic considerations. In the context of the Minkowski-Bouligand dimension,^{48–50}, a means of computing fractal dimension for the assessment of geometric structures, both have a standard dimension in \mathbb{R} of nq (agnostic to shape), which recalling from the Introduction is equivalent to nq . For $\mathbf{\Delta}$ and \mathbf{V} the standard dimension is nm , as our input vector m is of length m – but as mentioned these should not dominate calculations in realistic settings and it is quite simple to substitute their dimensions into subsequent results if so.

929

930

931

932

933

934

935

936

937

938

939

940

941

942

943

944

So our covering numbers for a matrix \mathbf{A} will be

945

$$N_\alpha^{cov}(\mathbf{B}) \leq \left(\frac{2\sqrt{\mathcal{IJ}\|\mathbf{A}\|_1\|\mathbf{A}\|_\infty}}{\alpha} \right)^{\mathcal{IJ}}$$

with \mathcal{IJ} used to denote the arbitrary dimensions so that calculations need not be repeated with each matrix. For convenience, we define $\tilde{\alpha} = \frac{1}{\alpha}$. The M-B dimension is then defined as

946

947

$$\dim_{MB}(X) = \limsup_{\tilde{\alpha} \rightarrow \infty} \frac{\log N_\alpha^{cov}}{\log(\tilde{\alpha})}$$

So once again using the general \mathbf{A} to represent either matrix of interest the M-B dimension of the matrices here is

948

949

$$\dim_{MB}(X) = \limsup_{\tilde{\alpha} \rightarrow \infty} \frac{\mathcal{IJ} \log \left(2\tilde{\alpha} \sqrt{\mathcal{IJ}\|\mathbf{A}\|_1\|\mathbf{A}\|_\infty} \right)}{\log(\tilde{\alpha})}$$

Expanding terms, we have

950

$$\dim_{MB}(X) = \limsup_{\tilde{\alpha} \rightarrow \infty} \frac{\mathcal{IJ} \left(\log(\tilde{\alpha}) + \log \left(2\sqrt{\mathcal{IJ}\|\mathbf{A}\|_1\|\mathbf{A}\|_\infty} \right) \right)}{\log(\tilde{\alpha})} = \mathcal{IJ}$$

So as we take the limit, the only term which remains is the product \mathcal{IJ} , our M-B dimension. 951
 This is not a novel result, but is included for clarity's sake in our usage of the bounding results 952
 from²². 953

For the Lipschitz constant \mathcal{K} , we need only note that the values of x cannot change faster 954
 than the rate of the fastest chemical process whose components are included in x . Because in 955
 most cases computational complexity will restrict us to some d -dimensional subset of the true 956
 d' -dimensional space of chemicals within the diseased region x' , we can define \mathcal{K} as 957

$$\mathcal{K} = \max_{q \in n} \min_{l \in \mathcal{L}_{qr}} \max_{t \in \mathcal{T}} \frac{dx_l}{dt} \quad (35)$$

where $t \in \mathcal{T}$ simply represents all time, q is an index in the state vector x and l is an 958
 index of the true d' -dimensional vector of chemical species. Put in words, if we have defined 959
 some element \mathbf{G}_{qr} such that it describes a multi-step process converting $x_r \rightarrow x_q$ via some 960
 intermediate sequence of chemicals with indices $l \in \mathcal{L}_{qr}$, the set of chemicals which exist in the 961
 true process of converting between x_r and x_q . Essentially, this tells us the rate of change in x_q 962
 is bounded from above by the rate of the slowest step in the true chemical process converting 963
 $x_r \rightarrow x_q$. This is critical, because chemical processes in living cells can have rates which range 964
 over multiple orders of magnitude. If we do not wish to consider intermediate steps, or if a given 965
 x_q and x_r pair are both in the vector x , then we can simply remove the minimization from the 966
 definition where relevant. 967

The mathematical definition is less clarifying than a verbal one in terms of the physical meaning. 968
 If we define some subset of biochemical processes as being "of interest", \mathcal{K} is essentially 969
 the fastest anything "of interest" could ever feasibly change within the volume.²² So the above 970
 optimization problem yields the Lipschitz constant for the entire model. 971

Eluder Dimension

From here, we use the definition of the "eluder dimension"²³ for the following analysis. Linear 973
 and quadratic matrix equations will be the function classes of interest here, and for the sake of 974
 generality we will use \vec{a} and \mathbf{A} to represent arbitrary vectors and matrices. 975

The eluder dimension of a function class \mathcal{F} is essentially the longest possible sequence of 976
 estimated states such that the next state is not revealed to within ϵ certainty. In the context of 977
 this study, \mathcal{F} is equivalent to a combination of 1) the transform between states and observations 978
 $\tilde{\mathbf{B}}$, and 2) the outcome for a given policy, as defined by the mathematical model derived in 979
 Supplemental Information Section 1. While our model is quadratic, the eluder dimension for 980
 quadratic transition processes was proven in²². 981

Put precisely, for a function class \mathcal{F} , some value $v \in \mathbf{Q}$ is (\mathcal{F}, ϵ) -dependent on $\{v_1, \dots, v_k\} \in \mathbf{Q}$ iff 982
 ϵ 983

$$\forall f, \tilde{f} \in \mathcal{F}, \sum_{i=1}^k \|f(v_i) - \tilde{f}(v_i)\|_2^2 \leq \epsilon^2 \implies \|f(v_i) - \tilde{f}(v_i)\|_2 \leq \epsilon$$

²²"Feasibly" is admittedly a somewhat unclear term without a lengthy discussion of bounding extremal cases. Suffice it to say that this restricts our discussion to the set of changes which can occur via biochemical means (interpreted loosely), while excluding various outliers like a physical ablation of a tumor, a sudden mass die-off event, or a meteor strike.

²³Whose form in the vector case was first presented in²².

As a further explanation, this can be summarized as stating that some sequence cannot be learned to $\leq \epsilon$ confidence within k samples using function class \mathcal{F} . The ϵ **eluder dimension** of \mathcal{F} , or $\dim_E(\mathbb{E}[\mathcal{F}], \epsilon)$, is the maximal k from the above definition such that v is not (\mathcal{F}, ϵ) -dependent on the sequence of k samples beforehand. Put simply, after k iterations we have learned a member of hypothesis function class \mathcal{F} such that given a known input, the expectation of the output would be known to within L2 norm ϵ error. If we consider the the number of measurements over which the following condition holds,

$$\forall f, f' \in \mathcal{F}, \|f(x) - f'(x)\| \leq \epsilon$$

The eluder dimension is the length of the longest possible sequence of measurements until this condition of ϵ -independence will no longer hold.

For a quadratic matrix function $\vec{a}^T \mathbf{A} \vec{a}$ with $\mathbf{A} \in \mathbb{R}^{\mathcal{I} \times \mathcal{I}}$ and $\forall k, \|\vec{a}(k)\| \leq \|\vec{a}(k)\|_{\max}$, the eluder dimension is

$$\dim_E(\mathbb{E}[\mathcal{F}], \epsilon_A) = \mathcal{O}\left(\mathcal{I}^2 \log\left[\frac{\mathcal{I}\|\mathbf{A}\|_1\|\mathbf{A}\|_\infty\|\vec{a}\|_{\max}}{\epsilon_A}\right]\right)$$

Substituting in the fact that the largest such \mathbf{A} in our model will be in $\mathbb{R}^{\mathcal{O}(n) \times \mathcal{O}(n)}$ and define functions of x , the eluder dimension of the model ψ will be

$$\dim_E(\mathbb{E}[\mathcal{F}], \epsilon_A) = \mathcal{O}\left(n^2 \log\left[\frac{n\|\mathbf{A}\|_1\|\mathbf{A}\|_\infty\|x\|_{\max}}{\epsilon_A}\right]\right)$$

Because there are multiple ways of formulating the problem without altering these bounds, as discussed in Section 1 of the Supplemental Information, we do not specify \mathbf{A} in terms of Δ , \mathbf{V} , Ξ , \mathbf{B} , \mathbf{G} . In each case, it will still hold that $\mathbf{A} \in \mathbb{R}^{\mathcal{O}(n) \times \mathcal{O}(n)}$, so it does not impact our analysis.

If we have a pre-set linear reward function $R(x(k), u(k))$ it will not factor into the regret bounds. However, we could suppose a situation in which the desired c are not known but there is some known desired output. In this case we would formulate it as a linear function of $\{x, u\}$ (a concatenation of x and u) defined by $\vec{\omega}$ such that

$$R(x(k), u(k)) = \vec{\omega}^T \{x, u\}$$

With $\vec{\omega}$ the function to be learned, the eluder dimension is

$$\dim_E(\mathbb{E}[\mathcal{F}], \epsilon_R) = \mathcal{O}\left((n + m) \log\left[\frac{\|\vec{\omega}\|_2\|\{x, u\}\|_{\max}}{\epsilon_R}\right]\right)$$

Regret Bounds

As stated in Equation (31) and Equation (30), the Bellman equation for our system is

$$V(x(k), u(k)) = \mathbb{E}[-\vec{\omega}x(k) - \vec{\mu}u(k)] + \gamma \int_{x' \in X} dx' \Psi(x, u) V(x'(k+1), u(k+1)) \quad (36)$$

Subject to the constraint that $\|u(k)\|_2 \leq \theta$. The expected regret out to a given time horizon is

$$\mathbb{E}[\tilde{\text{reg}}] = \sum_{k=k_0}^{\tau} [V_e(x(k), u(k)) - V_e(x(k), u^*(k))] \quad (37)$$

Which is the expectation value of the difference between the reward of a given policy $u(\cdot)$ 1009 versus the reward from an optimal policy $u^*(\cdot)$. 1010

Recall that $\psi(x, u)$ is equivalent to $\mathbb{E}[\Psi(x, u)]$ because the noise in Ψ is zero-mean, and so 1011 we use the former for simplicity given the expectation value is being studied here.²⁴ \mathcal{K} is the 1012 Lipschitz constant for the model, defined in Equation (35). Additionally, σ_ψ is the variance of the 1013 model's sub-Gaussian noise and σ_R is the equivalent for the instantaneous reward function. 1014

Thus, by the results of²², for desired expected error bounds of all ϵ with T the total time 1015 elapsed, for $\vec{\omega}$ and the largest parameter matrix (denoted as) \mathbf{A} , we obtain a regret bound of 1016

$$\mathbb{E}[\tilde{\text{reg}}](T, \Psi, R, \{\epsilon\}) = \tilde{\mathcal{O}}\left(\sqrt{T}\left(\sigma_R(m+n)\sqrt{\log\left[\frac{\|\vec{\omega}\|_2\|x, u\|_{\max}}{\epsilon_R}\right]} + \mathbb{E}[\mathcal{K}]\sigma_\psi n\sqrt{\log\left[\frac{n\|\mathbf{A}\|_1\|\mathbf{A}\|_\infty\|x\|_{\max}}{\epsilon_\psi}\right]}\right)\right) \quad (38)$$

The bounding convention $\tilde{\mathcal{O}}$, has been used instead of the standard \mathcal{O} to denote that we 1017 are ignoring two specific terms which are $\mathcal{O}\left(\sqrt{\dim_{\mathbb{E}}(\mathbb{E}[\mathcal{F}])\sqrt{\log(T)}}\right)$ with $\mathcal{F} = x^T \mathbf{A} x$ and $\mathcal{F} = 1018 R(x(k), u(k))$. 1019

This gives us our total regret bound for learning model parameters and (if relevant) the 1020 reward function using the PSRL algorithm discussed in^{22,23,47}. Our total regret grows as the \sqrt{T} , 1021 so the regret per unit time decays as $\frac{1}{\sqrt{T}}$, converging nicely. 1022

²⁴See the derivation given in Supplemental Information Section 1, and specifically the shorthand notation defined in Equation (27).

Supplemental Information 5: Statistical Properties of the Un- learnable Error $\vec{\varepsilon}$

Precise worst-case

We begin with the assumption that measurement errors are normally distributed and thus appear as Gaussian noise within the transition function. While some portion of the model's error can be reduced through the RL algorithm's improvement process, there remains a certain irreducible error component. This irreducible error has contributions from a number of factors discussed in the main text, resulting in a strict lower bound on the total model error.

We denote this unlearnable error component as $\vec{\varepsilon}$. For each parameter matrix in the final model equation, there is a corresponding error matrix that defines the unlearnable portion of each entry in that parameter matrix. We aim to define $\vec{\varepsilon}$ in a way that does not explicitly depend on the system state vector \mathbf{x} . Using H to denote the combined matrix associated with the linear term and A to denote the combined matrix for the quadratic term, we can describe the irreducible model error as follows:

$$\{H + v, A + \Upsilon\} \rightarrow \{H\mathbf{x} + v\mathbf{x}, \mathbf{x}^T A \mathbf{x} + \mathbf{x}^T \Upsilon \mathbf{x}\}$$

Since each v and Υ characterizes unlearnable contributions to H and A respectively, we represent the unlearnable vector $\vec{\varepsilon}$ as

$$\vec{\varepsilon} = v\mathbf{x} + \vec{1}\mathbf{x}^T \Upsilon \mathbf{x}$$

By nature of the model, we consider \mathbf{x} in terms of concentrations, satisfying $\|\mathbf{x}\| = 1$. This normalization implies a natural upper bound on $\vec{\varepsilon}$, since the worst-case alignment of \mathbf{x} with directions of v and Υ determines how large $\vec{\varepsilon}$ can become. The extreme case arises precisely if \mathbf{x} aligns with both $\|v\|_2$ and $\|\Upsilon\|_2$, causing them to reinforce each other completely, meaning we can likewise bound the expected value of $\vec{\varepsilon}$.

$$\vec{\varepsilon} \leq \vec{1}(\|v\|_2 + \|\Upsilon\|_2) \quad \text{for } n > 1,$$

$$\mathbb{E}[\vec{\varepsilon}] \leq \vec{1}\left(\frac{1}{n}\|v\|_2 + \|\Upsilon\|_2\right)$$

This supports the idea that it is possible to define a useful $\vec{\varepsilon}$ solely in terms of model error and not in any way in terms of \mathbf{x} .

Error Terms in Linear and Quadratic Forms

First, consider the linear term. Let H be the matrix associated with the linear portion of the model, and let $\vec{\varepsilon}$ be the unlearnable error vector. Then, for a state vector \mathbf{x} ,

$$H(\mathbf{x} + \vec{\varepsilon}) = H\mathbf{x} + H\vec{\varepsilon}$$

In this expression, $H\vec{\varepsilon}$ represents the unavoidable error contribution within the linear subproblem.

Next, we examine the quadratic term, captured by a matrix A . Writing the expansion of $(\mathbf{x} + \vec{\varepsilon})^T A(\mathbf{x} + \vec{\varepsilon})$, we have 1051
1052

$$\begin{aligned} (\mathbf{x} + \vec{\varepsilon})^T A(\mathbf{x} + \vec{\varepsilon}) &= \mathbf{x}^T A \mathbf{x} + \mathbf{x}^T A \vec{\varepsilon} + \vec{\varepsilon}^T A \mathbf{x} + \vec{\varepsilon}^T A \vec{\varepsilon} \\ &= \mathbf{x}^T A \mathbf{x} + \mathbf{x}^T (A + A^T) \vec{\varepsilon} + \vec{\varepsilon}^T A \vec{\varepsilon} \\ &\leq \|\mathbf{x}\|^2 \|A\|_2 + (\|A\|_2 + \|A^T\|_2) \|\mathbf{x}^T \vec{\varepsilon}\| + \|\vec{\varepsilon}\|^2 \|A\|_2 \end{aligned}$$

$$\begin{aligned} (\mathbf{x} + \vec{\varepsilon})^T A(\mathbf{x} + \vec{\varepsilon}) &= \mathbf{x}^T A \mathbf{x} + \mathbf{x}^T (A + A^T) \vec{\varepsilon} + \vec{\varepsilon}^T A \vec{\varepsilon} \\ &\leq \|\mathbf{x}\|^2 \|A\|_2 \cos \theta_{x, \|A\|_2} + (\|A\|_2 + \|A^T\|_2) \|\mathbf{x}^T \vec{\varepsilon}\| + \|\vec{\varepsilon}\|^2 \|A\|_2 \cos \theta_{\vec{\varepsilon}, \|A\|_2} \end{aligned}$$

Above, we use the fact that each sub-expression can be constrained by norms and alignment factors, and we can equivalently represent alignment factors via cosines. Putting the linear and quadratic components together, and then separating the terms representing contributions from the model errors gives the following: 1053
1054
1055
1056

$$H(\mathbf{x} + \vec{\varepsilon}) + \vec{1}(\mathbf{x} + \vec{\varepsilon})^T A(\mathbf{x} + \vec{\varepsilon}) = H\mathbf{x} + H\vec{\varepsilon} + \vec{1}(\mathbf{x}^T A \mathbf{x} + \mathbf{x}^T (A + A^T) \vec{\varepsilon} + \vec{\varepsilon}^T A \vec{\varepsilon})$$

$$\begin{aligned} H\vec{\varepsilon} + \vec{1}(\mathbf{x}^T (A + A^T) \vec{\varepsilon} + \vec{\varepsilon}^T A \vec{\varepsilon}) &\leq H\vec{1}(\|v\|_2 + \|\Upsilon\|_2) + \vec{1}(\mathbf{x}^T (A + A^T) \vec{1}(\|v\|_2 + \|\Upsilon\|_2) \\ &\quad + \vec{1}^T(\|v\|_2 + \|\Upsilon\|_2) A \vec{1}(\|v\|_2 + \|\Upsilon\|_2)) \end{aligned}$$

This bound arises from the fact that each $\vec{\varepsilon}$ term can be aligned with the corresponding largest singular directions, yielding the worst-case additive effect from the irreducible error vectors acting through H and A . 1057
1058
1059

Regret Bound at Time t

We're not worried about the presence of \mathbf{x} , focusing solely on the unavoidable portion of the model error. In particular, at a given time-step t , the expected contribution to regret from these unlearnable errors gives the following upper bound: 1060
1061
1062
1063

$$\begin{aligned} \mathbb{E}[\mathbf{reg}_{\vec{\varepsilon}}(t)] &\leq \left| \vec{\omega} \left(\|H\|_2 \vec{1} \left(\frac{1}{n} \|v\|_2 + \|\Upsilon\|_2 \right) + \vec{1} \left(\mathbf{x}(t)^T \|(A + A^T)\|_2 \vec{1} \left(\frac{1}{n} \|v\|_2 + \|\Upsilon\|_2 \right) \right. \right. \right. \\ &\quad \left. \left. \left. + \vec{1}^T \left(\frac{1}{n} \|v\|_2 + \|\Upsilon\|_2 \right) \|A\|_2 \vec{1} \left(\frac{1}{n} \|v\|_2 + \|\Upsilon\|_2 \right) \right) \right) \right| \end{aligned}$$

Equality occurs if all relevant directions align to maximize each error term. 1064

For clarity, a more explicit expression that allows for the direct analysis of these angles is 1065
the original form: 1066

$$\vec{\omega} H \vec{\varepsilon} + \vec{\omega} \vec{1} (x^T (A + A^T) \vec{\varepsilon} + \vec{\varepsilon}^T A \vec{\varepsilon}) \quad (39)$$

In the worst-case scenario, all directions are exactly identical, i.e., $\vec{\omega}$ and $H \vec{\varepsilon}$ are in the same 1067
direction, $\vec{\varepsilon}$ is in the same direction as the vector for $\|H\|_2$, \vec{x} is in the same direction as $(A + A^T) \vec{\varepsilon}$, 1068
 $\vec{\varepsilon}$ is in the same direction as $\|A + A^T\|_2$, $\vec{\varepsilon}$ is also in the same direction as $(A + A^T) \vec{\varepsilon}$, and $\vec{\varepsilon}$ is in 1069
the same direction as the vector for $\|A\|_2$. 1070

To get a realistic bound, it will be helpful to account for the spectral distributions of A and H . 1071
For example, the effects of each singular value of H on $\vec{\varepsilon}$ will be rescaled by the cosine of the 1072
angle between $\vec{\varepsilon}$ and that singular value's direction. A similar argument applies for A , especially 1073
when considering $(A + A^T)$, which has its own spectral structure. 1074

PDF Calculation 1075

Let X be a random vector uniformly distributed on the sphere $S^{n-1} \subset \mathbb{R}^n$. Here we have 1076
an $(n-1)$ -dimensional manifold, which is in \mathbb{R}^n rather than \mathbb{R}^{n-1} . A simple example is a circle, 1077
which can be parametrized by θ with polar coordinates, so it is a 1-manifold, yet the points on a 1078
circle are given with the 2-d coordinates (x, y) . The probability measure is the normalized $(n-1)$ - 1079
dimensional surface area measure on S^{n-1} . This means the entire sphere will have measure 1, 1080
and there is a surface area measure σ , and integrating a function f with respect to σ gives the 1081
notion of surface area \times some function value. To make σ a probability measure, it is necessary 1082
that $P(S^{n-1}) = 1$. 1083

$$P(A) = \frac{\sigma(A)}{\sigma(S^{n-1})}$$

for all measurable sets $A \subseteq S^{n-1}$. Then $P(A)$ is the probability that X lies in A . 1084

Without loss of generality, let v be a fixed unit vector in \mathbb{R}^n . We can make this assumption 1085
since scaling a non-zero reference vector to be unit length does not impact angle. Define the 1086
angle Θ between X and v by 1087

$$\Theta = \arccos(X \cdot v) \text{ and } 0 \leq \Theta \leq \pi$$

Note that Θ is taken to be the smaller angle between the two vectors, which justifies the 1088
given interval $[0, \pi]$. 1089

We wish to derive the probability density function of Θ in terms of the dimension n . Equiv- 1090
alently, this is the same as knowing how large a “slice” of the sphere corresponds to vectors at 1091
angle θ from v . This is only because we have X uniformly distributed on the sphere. 1092

Geometric Slicing Argument 1093

A point $X \in S^{n-1}$ is at an angle θ from v if and only if $X \cdot v = \cos(\theta)$. The set $\{X : X \cdot v = 1094$
 $\cos(\theta)\}$ is an $(n-2)$ spherical cap boundary, meaning it is a slice of the sphere of dimension 1095

$(n-2)$. The reason this is $(n-2)$ -dimensional is because the sphere itself is $(n-1)$ dimensional, and enforcing a linear condition ($X \cdot v = \cos(\theta)$) reduces the dimension by 1. A familiar example of this is the ordinary 2D sphere in three dimensional space, the set of points on S^2 satisfying $X \cdot v = \cos(\theta)$ is a circle S^1 which is 1-dimensional.

Consider a slice of the sphere corresponding to angles in $[\phi, \phi + d\phi]$. If we fix ϕ , the intersection $\{X : \Theta \approx \phi\}$ is an $(n-2)$ -dimensional sphere of radius $\sin(\phi)$ sitting in a plane orthogonal to v . The measure of that slice is

$$d(\text{Area}) \propto (\sin \phi)^{n-2} d\phi$$

It is easy to visualize this on the 3D sphere. Pick a "north pole" vector v , fix an angle, the condition where $X \cdot v = \cos(\phi)$ geometrically slices a $(n-2)$ -dimensional manifold. If one thinks about it in terms of a right triangle, $\|X\| = 1$, $X \cdot v = \|X\| \|v\| \cos(\phi) = \cos(\phi)$, so by the Pythagorean theorem, the distance orthogonal to v becomes $\sqrt{1 - \cos^2(\phi)} = \sin(\phi)$. Hence that slice is all of the vectors whose "height" is $\cos(\phi)$, living in an $(n-2)$ -dimensional space orthogonal to v , of radius $\sin(\phi)$.

In order to get the exact constant of proportionality, we impose an integral from 0 to π of that measure which equals the total surface area of S^{n-1} .

$$\int_0^\pi c(\sin \phi)^{n-2} d\phi = \text{Area}(S^{n-1}) = \frac{2\pi^{n/2}}{\Gamma(\frac{n}{2})}$$

We then use this known trigonometric integral identity to solve for c , and let $m = n - 2$.

$$\int_0^\pi (\sin \phi)^m d\phi = \frac{\sqrt{\pi} \Gamma(\frac{m+1}{2})}{\Gamma(\frac{m+2}{2})}, \quad m > -1$$

$$\int_0^\pi (\sin \phi)^{n-2} d\phi = \frac{\sqrt{\pi} \Gamma(\frac{n-1}{2})}{\Gamma(\frac{n}{2})}$$

$$c \frac{\sqrt{\pi} \Gamma(\frac{n-1}{2})}{\Gamma(\frac{n}{2})} = \frac{2\pi^{n/2}}{\Gamma(\frac{n}{2})} \Rightarrow c = \frac{2\pi^{n/2}}{\Gamma(\frac{n}{2})} \cdot \frac{\Gamma(\frac{n}{2})}{\sqrt{\pi} \Gamma(\frac{n-1}{2})} = \frac{2\pi^{\frac{n}{2}}}{\sqrt{\pi} \Gamma(\frac{n-1}{2})}$$

This integral is the total surface area. For the pdf of Θ we must normalize each ring's area by the total surface area using a normalized measure.

$$\frac{d(\text{surface area})}{\text{Area}(S^{n-1})} = \frac{c(\sin \phi)^{n-2}}{\text{Area}(S^{n-1})}$$

$$p_\Theta(\phi) d\phi = \frac{(\text{surface area of slice between angles } [\phi, \phi + d\phi])}{(\text{total surface area of } S^{n-1})}$$

Using this probability density function and our normalized measure, we can obtain the pdf of the angle Θ between a fixed unit vector v and a random uniformly distributed vector X on S^{n-1} .

$$p_\Theta(\phi) = \frac{c(\sin \phi)^{n-2}}{\text{Area}(S^{n-1})}$$

$$p_\Theta(\phi) = \frac{\frac{2\pi^{n/2}}{\sqrt{\pi}\Gamma(\frac{n-1}{2})}(\sin \phi)^{n-2}}{\frac{2\pi^{n/2}}{\Gamma(\frac{n}{2})}} = \frac{\Gamma(\frac{n}{2})}{\sqrt{\pi}\Gamma(\frac{n-1}{2})}(\sin \phi)^{n-2} \quad (40)$$

This completes the derivation of the pdf of Θ , the angle between a fixed unit vector and a random, uniformly distributed vector X on S^{n-1} . 1116
1117

Accounting For The Distribution of Angles

1118

We first note that H for the linear term, or A for the quadratic term, must have a singular value decomposition given as 1119
1120

$$H = U_H \Sigma_H V_H^T \quad (41)$$

where Σ_H is the diagonal matrix of singular values $\{\sigma_i(H)\}$, and U_H , V_H are orthonormal bases of \mathbb{R}^n capturing the left and right singular vectors. Acting on an error vector $\vec{\varepsilon}$ then yields $H\vec{\varepsilon}$. In the worst case, we would say that $\vec{\varepsilon}$ aligns perfectly with the top right singular vector $v_1(H)$ of H corresponding to the largest singular value, so that $\|H\vec{\varepsilon}\|$ achieves its maximum $\|H\|\|\vec{\varepsilon}\|$. In general, the true alignment factor is $\|\vec{\varepsilon}\| \cos(\theta_H)$ where θ_H is the angle between $\vec{\varepsilon}$ and $v_1(H)$. 1121
1122
1123
1124
1125

An analogous statement applies for the quadratic term $\vec{\varepsilon}^T A \vec{\varepsilon}$. In a worst-case sense, $\|\vec{\varepsilon}^T A \vec{\varepsilon}\|$ can reach $\|A\|\|\vec{\varepsilon}\|^2$ when $\vec{\varepsilon}$ aligns with the top eigenvector of the symmetric part of A . More realistically, one obtains a factor $\cos(\theta_A)$ that reduces the magnitude below its maximal value whenever $\vec{\varepsilon}$ is not perfectly aligned with that principal eigenvector. 1126
1127
1128
1129

From Equation (40) where the distribution of the angle θ is derived, one can see that typical values of $\cos(\theta)$ are small, especially in high dimensions n . Indeed, random vectors on the sphere in \mathbb{R}^n are very likely to be nearly orthogonal, which implies a large angle $\theta \approx \frac{\pi}{2}$. Consequently, the expectation $\mathbb{E}[\cos(\theta)]$ is significantly less than 1 as n grows. This is discussed further in the next section. 1130
1131
1132
1133
1134

Deriving a Tighter Bound

1135

A more realistic scenario than assuming $\|\vec{\varepsilon}\|$ always aligns with the top singular or eigen-directions is to include an angle θ_M for each matrix-vector pair. For instance, $\|H\vec{\varepsilon}\|$ is more realistically $\leq \|H\|_2 \|\vec{\varepsilon}\| \cos(\theta_H)$, and so on and so forth for the following terms. If we define $\theta_H, \theta_A, \dots$ for each of these matrix-vector pairs, in the worst case scenario each $\theta = 0$. More typically, $\mathbb{E}[\cos(\theta_M)] < 1$, where M are matrices A, H, \dots 1136
1137
1138
1139
1140

$$\mathbb{E}[\|H\vec{\varepsilon}\|] \leq \|H\|_2 \|\vec{\varepsilon}\| \mathbb{E}[\cos(\theta_H)]$$

$$\mathbb{E}[\vec{\varepsilon}^T A \vec{\varepsilon}] \leq \|A\|_2 (\|\vec{\varepsilon}\|^2) \mathbb{E}[\cos(\theta_A)]$$

$$\mathbb{E}[x^T (A + A^T) \vec{\varepsilon}] \leq \|A + A^T\|_2 \|\vec{\varepsilon}\| \|\mathbf{x}\| \mathbb{E}[\cos(\theta_{A,x})]$$

For multiple angles we just multiply the factor corrections, so if $\vec{\varepsilon}$ needs to align with a singular direction of H and simultaneously align with the top eigenvectors of A we then have the factor $\mathbb{E}[\cos(\theta_H) \cos(\theta_A)]$. 1141
1142
1143

We know $\vec{\varepsilon}$ is uniformly distributed over the unit sphere, and $\vec{\omega}$ is an external vector whose direction might be fixed, so we can't have distributional arguments for angles involving $\vec{\omega}$. The angles θ in question will then admit the distribution derived in Equation (40). 1144
1145
1146

$$\begin{aligned} & |\vec{\omega} H \vec{\varepsilon}| \cos(\theta_{\vec{\omega}, H \vec{\varepsilon}}) \\ & ||\vec{\omega}|| \cos(\theta_{\vec{\omega}, \vec{1}}) \cdot \left(||\vec{\varepsilon}| \cos(\theta_{x, (A+A^T)\vec{\varepsilon}}) \right) \\ & ||\vec{\omega}|| \cos(\theta_{\vec{\omega}, \vec{1}}) \cdot \left(||\vec{\varepsilon}|^2 \cos(\theta_{\vec{\varepsilon}, A\vec{\varepsilon}}) \right). \end{aligned}$$

Recall Equation (41), then for a vector $\vec{\varepsilon} \in \mathbb{R}^n$ 1147

$$H \vec{\varepsilon} = \sum_{i=1}^n \sigma_i(H) \langle \vec{\varepsilon}, w_i(H) \rangle u_i(H)$$

with $w_i(H)$ the columns of W_H and $u_i(H)$ the columns of U_H . For an isotropic $\vec{\varepsilon}$ on the sphere, each $\langle \vec{\varepsilon}, w_i(H) \rangle$ behaves like a mean-zero random variable with variance depending on $\|\vec{\varepsilon}\|$. Summing up these contributions provides 1148
1149
1150

$$\|H \vec{\varepsilon}\|^2 = \left\| \sum_{i=1}^n \sigma_i(H) \langle \vec{\varepsilon}, w_i(H) \rangle u_i(H) \right\|^2.$$

$\|H \vec{\varepsilon}\| \leq \|H\| \|\vec{\varepsilon}\|$ in the extreme alignment case, and more generally one obtains 1151

$$\|H \vec{\varepsilon}\| \leq \|H\| \|\vec{\varepsilon}\| \cos(\theta_H)$$

which reflects a partial rather than full worst-case alignment. 1152

Now, for the $\mathbf{x}^T (A + A^T) \vec{\varepsilon}$ term, \mathbf{x} is unit length so we can skip that factor. We decompose $(A + A^T)$ via SVD or spectral decomposition, and let $\{v_i\}_{i=1}^n$ be singular values of $(A + A^T)$. Let $\{u_i\}$ and $\{w_i\}$ be the left and right singular vectors respectively. It follows that 1153
1154
1155

$$(A + A^T) \vec{\varepsilon} = \sum_i v_i \langle \vec{\varepsilon}, w_i \rangle u_i$$

The direction $\vec{\varepsilon}$ in the basis of $\{w_i\}$ can be random if $\vec{\varepsilon}$ is isotropic, so $\langle \vec{\varepsilon}, w_i \rangle$ is a random scalar with zero mean and distribution consistent with uniform direction on the sphere. The sum $\mathbf{x}^T (A + A^T) \vec{\varepsilon}$ becomes 1156
1157
1158

$$\mathbf{x} \cdot \sum_i v_i \langle \vec{\varepsilon}, w_i \rangle u_i = \sum_i v_i \langle \vec{\varepsilon}, w_i \rangle (\mathbf{x} \cdot u_i)$$

Each term has its own angle factor, so overall, we get a random sum of the form $\sum_i v_i \varepsilon_i$, if you rename $\varepsilon_i = \langle \vec{\varepsilon}, w_i \rangle$ and some weighting from $\mathbf{x} \cdot u_i$. 1159
1160

Now we consider the $\vec{\varepsilon}^T A \vec{\varepsilon}$ term. If we consider the singular value decomposition of A ,

1161

$$A = U_A \Sigma_A W_A^T$$

By a similar argument to $\|H\vec{\varepsilon}\|$, one has

1162

$$|\vec{\varepsilon}^T A \vec{\varepsilon}| \leq \|A\| \|\vec{\varepsilon}\|^2 \cos(\theta_{\vec{\varepsilon}, A \vec{\varepsilon}})$$

It is important to see that the final expression we get is a sum of sub terms, each with an alignment factor. The naive bound will lump all of these to equal one, but in our case, we have a cosine term.

1163

1164

1165

We define the worst-case regret expression where all of our cosine factors become 1, giving

$$\text{reg}_{\vec{\varepsilon}}^{(\text{worst})} := |\vec{\omega} H \vec{\varepsilon}| + \|\vec{\omega}\| (\|\vec{\varepsilon}\| + \|\vec{\varepsilon}\|^2).$$

In the actual scenario, the alignment angles θ are not always zero, each term is multiplied by a corresponding cosine factor

1166

1167

$$\text{reg}_{\vec{\varepsilon}}^{(\text{actual})} := |\vec{\omega} H \vec{\varepsilon}| \cos(\theta_{\vec{\omega}, H \vec{\varepsilon}}) + \left[\|\vec{\omega}\| \cos(\theta_{\vec{\omega}, \vec{1}}) \right] \left(\|\vec{\varepsilon}\| \cos(\theta_{x, (A+A^T) \vec{\varepsilon}}) + \|\vec{\varepsilon}\|^2 \cos(\theta_{\vec{\varepsilon}, A \vec{\varepsilon}}) \right)$$

Because $|\vec{\omega}| \cos(\theta_{\vec{\omega}, \vec{1}})$ is a value specified by the user, it can be treated as a constant when doing statistical analysis. It thus may be easier to think of it as some $g(\vec{\omega}) = |\vec{\omega}| \cos(\theta_{\vec{\omega}, \vec{1}}) = \varphi$. Thus, our regret term can be expressed as:

1168

1169

1170

$$\text{reg}_{\vec{\varepsilon}}^{(\text{actual})} = |\vec{\omega} H \vec{\varepsilon}| \cos(\theta_{\vec{\omega}, H \vec{\varepsilon}}) + \varphi \|\vec{\varepsilon}\| \cos(\theta_{x, (A+A^T) \vec{\varepsilon}}) + \varphi \|\vec{\varepsilon}\|^2 \cos(\theta_{\vec{\varepsilon}, A \vec{\varepsilon}})$$

One can observe that each of the three remaining cosine factors depends on one or two uniformly distributed directions in \mathbb{R}^n . Because these directions are isotropic on the sphere, their distributions are isomorphic under the action of $\text{SO}(n)$ (i.e., any rotation on the n -sphere). As a result, one can apply a suitable rotation so that the first vector in each pair is aligned, while the second vector remains isotropic. This transformation causes the probability distributions for all three cosines to be identical.

1171

1172

1173

1174

1175

1176

Thus, in the specific scenario where we regard these angles as random and identically distributed, it suffices to introduce a single random angle $\theta \in [0, \pi]$. This leads us to the following expression for the distribution of regret from unlearnable error:

1177

1178

1179

(42)

Where $\varphi = \|\vec{\omega}\| \cos(\theta_{\vec{\omega}, \vec{1}})$ is a constant set by the user, and θ is a single representative angle capturing the common isotropic distribution of those alignment factors.

1180

1181

When you compare the actual sum of sub-terms vs worst case sum of sub terms, it is clear to see

1182

1183

$$\frac{\text{reg}_{\vec{\varepsilon}}^{(\text{actual})}}{\text{reg}_{\vec{\varepsilon}}^{(\text{worst})}} = \cos(\theta)$$

$$\text{reg}_{\bar{\varepsilon}}^{(\text{actual})} = \text{reg}_{\bar{\varepsilon}}^{(\text{worst})} \cos(\theta) \quad (43)$$

This follows when we treat the multiple angle factors as identical, which is accurate up to rotation symmetries in high dimensions. Now, we apply the "blessing of dimensionality", and find the variance of the cosines of θ . 1184
1185
1186

A random uniform unit vector $U \in S^{n-1} \subset \mathbb{R}^n$ can be generated by sampling a standard normal vector $X \sim \mathcal{N}(0, I_n)$ and then normalizing $U = \frac{X}{\|X\|}$. Likewise, another independent unit vector V is obtained from an independent normal Y . By construction, 1187
1188
1189

$$\langle U, V \rangle = \frac{\langle X, Y \rangle}{\|X\| \cdot \|Y\|}$$

Because X and Y are standard normal and independent, $\langle X, Y \rangle$ has mean zero and variance on the order of $\|X\| \|Y\|$. As $n \rightarrow \infty$, we have $\|X\| \approx \sqrt{n}$ almost surely, and the same for $\|Y\|$. It follows that $\langle X, Y \rangle / \sqrt{n}$ becomes approximately a normal random variable with mean 0 and variance 1, by CLT. Hence, 1190
1191
1192
1193

$$\langle U, V \rangle \xrightarrow[n \rightarrow \infty]{d} \frac{Z}{\sqrt{n}}, \quad Z \sim \mathcal{N}(0, 1) \quad (44)$$

So the dot product is typically of order $1/\sqrt{n}$. For any $\varepsilon > 0$, the probability $|\langle U, V \rangle| \geq \varepsilon$ goes to zero as $n \rightarrow \infty$. Additionally, recall that $\langle U, V \rangle = \cos(\Theta)$ is the angle between U and V , so $\cos(\Theta) \approx 0 \implies \Theta \approx \frac{\pi}{2}$. Thus in high dimension, random unit vectors tend to be orthogonal with high probability. 1194
1195
1196
1197

We have found that $\mathbb{E}[\langle U, V \rangle] = 0$, so $\cos(\Theta)$ is centered near 0. The variance of $\cos(\Theta)$ is on the order of $1/n$, since $\langle U, V \rangle = \cos(\Theta)$, and for large n , $\text{Var}(\langle U, V \rangle) \approx \text{Var}\left(\frac{Z}{\sqrt{n}}\right) = \frac{1}{n}$. Because $\Theta \approx \frac{\pi}{2} - \cos(\Theta)$ for small $\cos(\Theta)$, we can do a small-angle approximation. For Θ near $\frac{\pi}{2}$, let $\Theta = \frac{\pi}{2} - \delta$. Then $\cos(\Theta) = \sin(\delta) \approx \delta$ (for small δ) so $\delta \approx \cos(\Theta) \approx \frac{Z}{\sqrt{n}}$. Hence, the angle's deviation δ from $\frac{\pi}{2}$ scales like $O\left(\frac{1}{\sqrt{n}}\right)$, and variance of δ is then on the order of $\frac{1}{n}$. 1198
1199
1200
1201
1202

$$\Theta \approx \frac{\pi}{2} \pm O\left(\frac{1}{\sqrt{n}}\right) \text{ with high probability as } n \text{ increases.}$$

We have thus demonstrated that our actual regret function is much tighter than our worst-case. Define $\mathcal{C} = \cos(\theta)$. With $\mathbb{E}[\mathcal{C}] = 0$ and $\text{Var}(\mathcal{C}) = \frac{1}{n}$, we have shown: 1203
1204

$$\mathbb{E}[\text{reg}_{\bar{\varepsilon}}^{(\text{actual})}] = \text{reg}_{\bar{\varepsilon}}^{(\text{worst})} \cdot \mathbb{E}[\mathcal{C}] \quad \text{with} \quad \mathbb{E}[\mathcal{C}] \ll 1 \quad \text{with high probability for large } n.$$

A Sketch of an Experimental Protocol

1205

While this paper is predominantly focused on the technical, mathematical aspects of the 1206 problem, our goal is for this work to have a near-term and direct pathway to practical application. 1207 Before this can be done there is a need for additional work extending this paper to address 1208 related problems which are beyond the scope of this paper. Such problems include initialization 1209 of the model from existing experimental data, determining sample sizes needed for a given 1210 experimental application, and other aspects of bridging our results to direct implementation. 1211

However, even though the precise technical details of our methods and results are likely to 1212 be approachable only for those with significant quantitative backgrounds, one of our core goals in 1213 the paper is for at least the gestalt of our results to be approachable to those from experimental 1214 biomedical research backgrounds. To that end, in this section we will briefly sketch out a rough 1215 framework for applying this method to experiments. 1216

In bullet-point format, the overall process would be thus: 1217

1. Determine which biomedical system²⁵ is to be studied. 1218
2. Describe quantitatively the initial conditions and goal conditions in terms of either biomarkers 1219 or relative frequencies of cell types. Additionally determine the time horizon over which 1220 this system is meant to be controlled. 1221
3. Compile existing and available relevant data on biochemical processes, transport processes, 1222 and other biophysical and cellular physiology aspects of the system to be studied. 1223
4. Apply an algorithm (beyond the scope of this paper) to convert this data into an initial model, 1224 so that our algorithm can start from an empirically supported model and thus operate more 1225 efficiently. 1226
5. Repeat (a)-(e) below until a desired level of performance in controlling the biomedical system 1227 is achieved, or the results are no longer improving at a rate considered worth the cost 1228 and time of additional experiments. 1229
 - (a) Run our approach's control algorithm to determine its prediction of inputs. This is 1230 determined from the goal conditions and the current model of the system. 1231
 - (b) Take its predictions for optimal inputs, and apply them to the system. 1232
 - (c) Either at the end of a given experiment, or intermittently throughout an experiment, 1233 feed the current output data from the system (as defined by the experimenters in step 1234 above) into the reinforcement learning (RL) algorithm used in our method. 1235
 - (d) The RL algorithm compares the differences between its predictions and the actual 1236 experimental outputs. 1237
 - (e) The RL algorithm updates its model of the system. 1238
6. Analyze the final performance, and apply to problems of interest the model produced by 1239 our method. 1240

A visual summary is provided in the figure. 1241

²⁵The clearest application is to evolutionary processes. However, thanks to our method's suitability for controlling ecological processes, broadly interpreted (e.g. intercellular and intracellular dynamics even in the absence of evolution), other applications may be feasible.

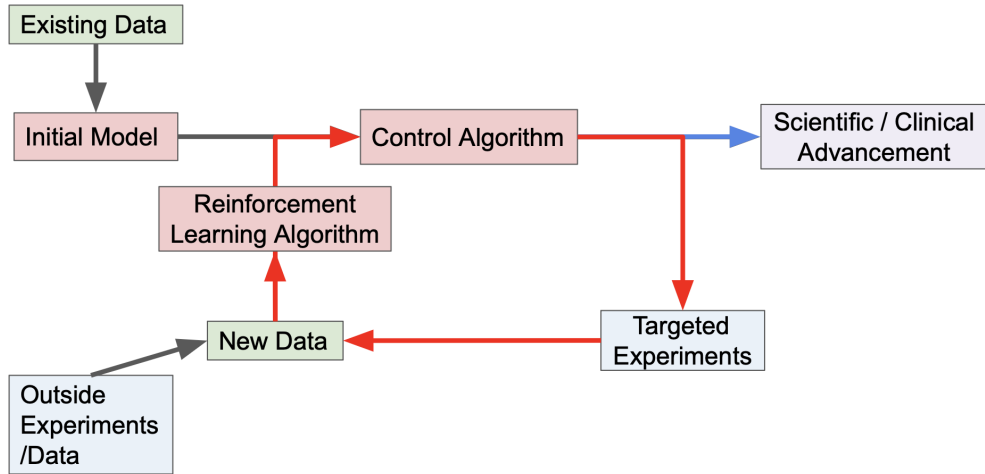


Figure 1: A visual summary of the sketch of an experimental protocol, described above. Red arrows denote the loop described in step 5 of the protocol sketch.

As noted previously, this is not a thorough protocol at a level used in experimental work. Instead, it is essentially a framework for constructing a thorough protocol, and is meant to help clarify the overall approach of this paper and support collaborations between quantitative researchers and experimental researchers.

1242

1243

1244

1245